

**Development of a mass spectrometry based method for the
identification of gp96-chaperoned peptides destined for
presentation in MHC class I molecules**

by

Angela M. Jackson
B.Sc., University of Victoria 2002

A Thesis Submitted in Partial Fulfillment of the Requirements for the Degree of

MASTER OF SCIENCE

In the Department of Biochemistry and Microbiology

© Angela Jackson, 2006
University of Victoria

All rights reserved. This thesis may not be reproduced in whole or in part, by photocopy or other means, without the permission of the author.

**Development of a mass spectrometry based method for the
identification of gp96-chaperoned peptides destined for
presentation in MHC class I molecules**

by

Angela M.Jackson
B.Sc., University of Victoria, 2002

Dr. T.W. Pearson (Supervisor)

Dr. A. Boraston (Department Member)

Dr. R. Burke (Department Member)

Dr. P. von Aderkas (Outside Member)

Supervisory Committee

Supervisor

Dr. T. W. Pearson

Departmental Member

Dr. A. Boraston

Departmental Member

Dr. R. Burke

Outside Member

Dr. P. von Aderkas

ABSTRACT

Theileria parva is an intracellular protozoan parasite and the causative agent of the lethal livestock disease East Coast fever (ECF). Research has shown that a protective cell-mediated immune response against parasite-infected lymphocytes is capable of clearing the host of *T. parva* (Pearson et al. 1979), leaving the host solidly immune to reinfection. The work presented in this thesis describes my attempts to develop a method for identification of major histocompatibility complex class I-associated *T. parva* peptides involved in eliciting this protective cell-mediated immune response.

The soluble chaperone gp96 interacts with peptides destined for association with major histocompatibility complex class I molecules and is therefore a source of *T. parva* peptides that interact with extracellular immune effectors. Using sensitive mass spectrometry methods the gp96-chaperoned peptide proteome from model parasite infected T lymphocytes was compared to an uninfected T cell line. With our findings we have demonstrated proof of concept for a highly sensitive method for the elucidation of potentially immunogenic peptides capable of initiating a protective immune response against the intracellular parasite *T. parva*.

TABLE OF CONTENTS

<i>SUPERVISORY COMMITTEE</i>	ii
<i>ABSTRACT</i>	iii
<i>TABLE OF CONTENTS</i>	iv
<i>LIST OF FIGURES</i>	vii
<i>LIST OF TABLES</i>	ix
<i>ACKNOWLEDGEMENTS</i>	x
CHAPTER 1. INTRODUCTION	
History of East Coast fever	1
The disease: pathogenesis and recovery	3
Disease control	4
Life cycle of <i>T. parva</i> in both vector and host	7
Cell mediated immunity	9
Antigen processing	10
CHAPTER 2. ENRICHMENT OF MOLECULES OF THE BOVINE ANTIGEN PROCESSING PATHWAY FOR DERIVATION OF MONOCLONAL ANTIBODIES.	
<i>INTRODUCTION</i>	12
<i>MATERIALS AND METHODS</i>	
2.1 Preparation of bovine liver glycoproteins	16
2.2 One-dimensional gel electrophoresis	17
2.3 Two-dimensional gel electrophoresis	18

2.4	Staining of proteins with colloidal Coomassie Brilliant Blue G-250	19
2.5	Derivation of monoclonal antibodies	20
2.6	Enzyme-linked immunosorbent assay	22
2.7	Immunoblotting	22
2.8	Dot blotting	23
2.9	Sample preparation for MALDI-TOF mass spectrometry	23
2.10	MALDI-TOF mass spectrometry	24

RESULTS

- Enrichment and identification of major glycoproteins from bovine liver tissue 26
- Derivation and characterization of monoclonal antibodies to enriched bovine liver glycoproteins 35

DISCUSSION 44

CHAPTER 3. IMMUNOAFFINITY ISOLATION OF BOVINE LIVER GP96 AND IDENTIFICATION OF BOUND PEPTIDES.

INTRODUCTION 48

MATERIALS AND METHODS

3.1	Affinity purification of gp96 from Murine EL4, Human Jurkat and <i>Theileria parva</i> -infected bovine lymphocytes	55
3.2	Immunoblotting	57
3.3	Peptide elution and reversed phase C18 column chromatography	58
3.4	iTRAQ™ peptide derivitization	58
3.5	Peptide fractionation by reversed phase chromatography	59
3.6	Tandem mass spectrometry	59
3.7	Database searching	60
3.8	Micro-dot blotting	60

<i>RESULTS</i>	
• Affinity purification of gp96 from <i>Mus musculus</i> EL4 cell line	62
• Optimization of MALDI TOF/TOF CHCA matrix	64
• Optimization of MALDI TOF/TOF fragmentation of iTRAQ™ labeled peptides	70
• Differential labeling and peptide sequence identification using a MALDI TOF/TOF analyzer	72
• Analysis of anti-gp96 ScFv species specificity	75
<i>DISCUSSION</i>	78
SUMMARY AND CONCLUSIONS	83
<i>APPENDIX I.</i> List of abbreviations	88
<i>APPENDIX II.</i> Alignment of endoplasmic reticulin glycoproteins from bovid and mouse	91
<i>APPENDIX III.</i> Alignment of bovid and <i>T. parva</i> gp96	94
<i>BIBLIOGRAPHY</i>	95

LIST OF FIGURES

FIGURE 2.1	Enrichment of glycoproteins from bovine liver cells	26
FIGURE 2.2	Profile of bovine liver glycoproteins eluted isocratically from a Con A affinity column	28
FIGURE 2.3	Immunoblot analysis of glycoprotein fractions from Con A affinity chromatographic separation of bovine liver proteins	29
FIGURE 2.4	RP-HPLC elution trace of molecules from Con A isolated bovine liver glycoproteins	31
FIGURE 2.5	Two-dimensional polyacrylamide gel analysis of fractionated glycoproteins from bovine liver tissue	33
FIGURE 2.6	ELISA titration of mouse antisera raised against bovine liver glycoproteins prior to <i>in vitro</i> antigen stimulation of lymphocytes and cell fusion	35
FIGURE 2.7	Dot blot analysis of monoclonal antibodies raised against bovine liver glycoproteins (hybridomas derived after <i>in vitro</i> antigen stimulation)	37
FIGURE 2.8	Immunoblot analysis of monoclonal antibodies	39
FIGURE 2.9	ELISA titration of mouse antisera raised against bovine liver glycoproteins prior to <i>in vivo</i> antigen stimulation of lymphocytes and cell fusion	40

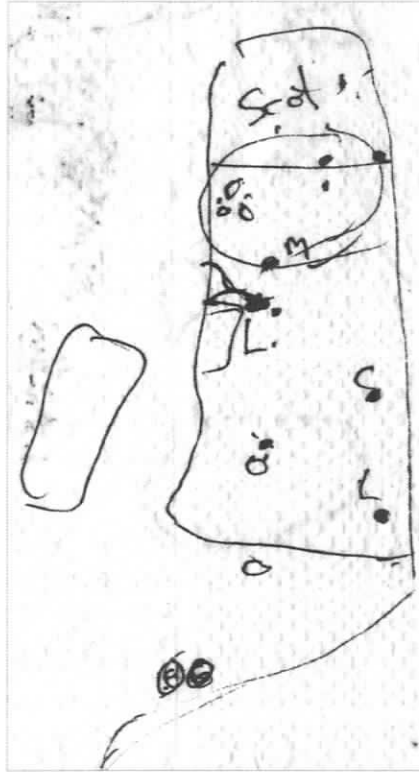
FIGURE 2.10 Immunoblot analysis of monoclonal antibodies produced after <i>in vivo</i> antigen stimulation	41
FIGURE 2.11 Specificity analysis of monoclonal antibodies derived after both <i>in vitro</i> and <i>in vivo</i> immunization methods	42
FIGURE 3.1 Immunoblot analysis of gp96 ScFv affinity purified from <i>Mus musculus</i> EL4 cell line	62
FIGURE 3.2 Optimization of MALDI TOF/TOF CHCA matrix concentration	64
FIGURE 3.3 Effects of ammonium citrate addition to MALDI TOF/TOF CHCA matrix	66
FIGURE 3.4 Optimization of MALDI TOF/TOF sample and CHCA matrix deposition technique	68
FIGURE 3.5 Optimization of MALDI TOF/TOF fragmentation of iTRAQ™ labeled BSA peptides	70
FIGURE 3.6 Differential labeling and peptide sequence identification using a MALDI TOF/TOF analyzer	72
FIGURE 3.7 Micro-dot blot analysis of anti-gp96 ScFv species specificity	75

LIST OF TABLES

TABLE 2.1	Mass spectrometric identification of bovine liver glycoproteins resolved by two-dimensional gel electrophoresis	34
TABLE 2.2	Summary: monoclonal antibodies produced against bovine liver glycoproteins	43
TABLE 3.1	Summary of identified iTRAQ™ labeled peptides, determination of their <i>de novo</i> sequence and their identity obtained using BLAST and MASCOT algorithms	74

ACKNOWLEDGEMENTS

I would like to thank my supervisor Dr. Terry Pearson for direction....



An example from the collection of maps drawn on Tim Horton napkins by Terry Pearson portraying his exemplary ability to give directions. Map is of the UK with emphasis on the Lake District north of Manchester...obviously!

somehow I made it through!

Faced with heaps of experiments and somewhat smaller heaps of results you navigated me through this degree with capability, humor and patience. You fill your lab with brilliant researchers whom I've had the pleasure to work alongside. Lee, you live the ideal that science is not bound by the walls of the lab; a moral value that has incited many animated lab conversations throughout the years. Along with those great debates I can't thank you enough for the chocolate that was so aptly on hand to soothe experimental

disappointments. Jody, you were the first person to convince me to pursue another degree, I wouldn't be here if you hadn't given me the idea in the first place. Jamie, you attack both life and science with passion; your excitement is contagious and will always make me smile. Emily thanks for suffering through this alongside me. To all of you, thank you for making this degree such a rewarding experience.

Of course this is not solely my work; many others played a role. I would like to thank the members of my committee, Dr. Allistair Boraston, Dr. Robert Burke and Dr. Patrick von Aderkas for their time and interest in this research. Thank you to my collaborator Christian Kleist at the University of Tübingen, Germany for providing me with the anti-gp96 ScFv antibody. I am indebted to Dr. Brett Poulis for chromatography equipment, HPLC tutorials and copious amounts of coffee. Rob Beecroft and Teri Otto of ImmunoPrecise Antibodies Ltd., thank you for assistance in monoclonal antibody derivation. Your knowledge is vast. To the members of the UVic Proteomics Center, thank you for your willingness to take both this project and grad student under your wing. Derek Smith, Darryl Hardie, Monica Elliot and Leanne Ohlund: a simple thank you for your MS expertise and guidance is a true understatement. Albert Labossiere, Scott Scholz and Steve Horak: thank you for technical assistance, equipment maintenance and non-scientific conversations. Deb Penner and Melinda Powell you are always smiling and ever knowing even when I appear to be asking skill testing questions- thank you.

To my long time friend Breena, thank you. You have kept me sane by opening my eyes to the humor that surrounds me everyday and when that isn't enough to deflect sure insanity you are my psychologist. To Steve, my husband and biggest fan, I strive to be that great human you see in me. Time has been a highly prized commodity during the past few years but you never made me choose between my education and the rest of my life. Thank you for being patient. Mom you never question my capabilities and wonder why I do. You empower me, believe in me and I love you. Steve, Breena and Mom, this is what I have been doing for the last few years...

CHAPTER 1. INTRODUCTION

HISTORY OF EAST COAST FEVER

Approximately 73 million people will be added to the world's population every year from now until 2020. Much of this population growth will occur in cities of the developing world where neither meat nor cereal production is keeping pace with demand (Pinstrup-Anderson 1999; Rosegrant and Cline 2003). In Africa the major constraint to agricultural growth is the prevalence of high mortality livestock diseases such as trypanosomiasis, Redwater and East Coast fever (ECF). ECF has a great impact on cattle in southern, eastern and central Africa where a century after its identification it still amasses losses exceeding \$ 180 million per annum (Dolan 1999). This economically important disease is caused by the parasite *Theileria parva*, which is found in 11 countries of sub-Saharan Africa. It is estimated that 24 million head of cattle are at risk for ECF, while one million animals succumb to the disease annually; two animals per minute (Macdonald-Levy 2005).

Historically, the emergence of ECF in Africa is entwined with Rinderpest, a viral livestock disease causing comparable mortality. It is estimated that in South Africa from 1896-1898, ninety percent of domestic cattle perished from Rinderpest infection (Dolan 1999; Norval 1992). The economic and social damage caused by the Rinderpest-devastated cattle herds prompted governments to develop strategies for livestock repopulation. Southern and central Africa imported livestock from such diverse areas as

Argentina, the United States of America and Madagascar (Dolan 1999; Norval 1992). In 1901 small numbers of cattle were also shipped from German East Africa (Tanganyika, now Tanzania) and with them the parasite responsible for ECF was introduced into South and central Africa (Dolan 1999; Norval 1992). The primary tick vector for the parasite in eastern Africa, *Rhipicephalus appendiculatus*, was also indigenous to southern and central Africa; in 1902 the deadly disease took hold in epidemic proportions (Cranefield 1991).

Despite the antiquity of the disease, ECF continues to cause extensive cattle loss into the 21st century. Control of the vector has environmental implications while adequate management of the parasite is plagued by the complexity of its lifecycle. Cattle that survive a *T. parva* infection are known to be immune to further homologous challenge. Therefore, immunization with nonviable *T. parva* antigens to prime the host immune system should provoke a protective response to field challenge. To devise such a vaccine for ECF requires a greater understanding of the interaction between *T. parva* and the bovine immune system. More specifically, the parasite immunogens provoking a protective immune response in the host need to be elucidated to control this economically crippling disease.

THE DISEASE: PATHOGENESIS & RECOVERY

The survival of a parasite species is adversely affected by reduced transmission; a consequence of inducing rapid host mortality. Through thousands of years of natural selection, successful host-parasite relationships evolve, balancing parasite transmission with host mortality. The indigenous African Cape buffalo (*Syncerus caffer*) have developed an innate resistance to *T. parva* and are believed to be its natural or principal host (Uilenberg et al. 1993). The Cape buffalo is an asymptomatic carrier of *T. parva* and serves as a parasite reservoir for the tick vector population. Unfortunately, common grazing ground used by both the Cape buffalo and cattle allows the tick vector to transmit *T. parva* to uninfected domestic livestock. Domestic cattle are permissive hosts for *T. parva* and suffer from a rapid onset, lymphoproliferative disease with high mortality. In addition, it has been shown that cattle that recover from ECF also serve as *T. parva* carriers, further complicating attempts to eradicate the disease (McKeever and Morrison 1998).

All *T. parva* strains live intracellularly within bovine T-lymphocytes and induce a reversible host cell transformation and metastatic phenotype (Dobbelaere et al. 2000). Infected livestock succumb to a leukemia-like death 2-4 weeks after infection (Heussler et al. 2002). The disease manifestations of *T. parva* infected cattle are a direct result of the clonal expansion of the parasitized cells, reminiscent of invasive malignant tumors. This lymphoproliferative phenotype has been termed “parasite-induced reversible transformation” because the parasitized cells can be induced to revert back to quiescent lymphocytes with long term tetracycline treatment (Association 1998b). This implies

that the parasite-induced alterations are not permanent and the host cell genome is left unmodified (Dobbelaere et al. 2000).

Clinically, the disease is characterized by enlargement of the superficial lymph nodes 7-10 days after attachment of the *T. parva* infected tick (Association 1998a; Pearson 1986). Susceptible cattle develop a high fever that is sustained throughout the course of the disease. This is accompanied by anorexia and nasal discharge as the infection disseminates (Pearson 1986). Severe pulmonary edema causes labored breathing during the terminal stages of the disease. Autopsy reveals widespread lymphocytolysis and haemorrhaging of affected organs as the animals succumb to the parasite infection (Kaufmann 1996).

DISEASE CONTROL

Despite the barrier imposed by ECF on Africa's agriculture growth, eradication of the disease appears to be an unrealistic goal. As long as African Cape buffalo (the natural *T. parva* host) and susceptible livestock share grazing land, the resident tick population will transmit the disease. Control of ECF is therefore the only practical option. The acaricide family of pesticides is used to control ECF at the vector level. An aqueous acaricide solution is applied to susceptible cattle by dipping or spraying. In areas where ticks are endemic, biweekly acaricide application can cost farmers \$ 20 US per animal per year (Norval 1992). Unfortunately the most important natural predator of *R. appendiculatus* is the oxpecker, a small bird (*Buphagus spp.*) which is also adversely affected by acaricide use. The numbers of oxpeckers that feed directly off the ticks attached to larger

herbivores have decreased substantially over the last decade due to acaricide poisoning (Norval 1992). Recently, pesticide contamination of human food and water sources also has been described (Bishop et al. 2002). Stringent application of the anti-tick pesticides has failed to eradicate *R. appendiculatus* and instead has resulted in increasing acaricide resistance in the tick population (Norval 1992).

Alternatively, control of ECF at the parasite level alleviates the environmental costs associated with acaricide use. Immunizing young calves with live *T. parva* sporozoites in conjunction with a long-acting oxytetracycline antibiotic is referred to as the infection and treatment (I and T) method of ECF control (Marcotty et al. 2002). The procedure uses cryopreserved stabilates of *T. parva* sporozoites obtained from infected ticks for inoculation. The necessary viability of the sporozoite inoculant requires cold storage, a luxury not available in many outlying areas affected with ECF. In regions where the treatment can be properly administered, the cost of \$ 40 per adult animal is prohibitive to smallholder cattle farmers (Norval 1992). For more affluent livestock operations, the protection offered by the I and T method is life long but restricted to homologous strains of ECF. Immunizing cattle with multiple strains of *T. parva* to confer a more complete protection against a variety of antigenically different strains of ECF can result in cattle having a multiple carrier status. It is important to recognize that persistent transmissible infection could disseminate non-native *T. parva* strains into the resident tick population.

Vaccinating livestock with intact, infective *T. parva* sporozoites jeopardizes the nativity of the resident tick population with nonnative strains of *T. parva*. An improvement over

the I and T method of ECF control could be achieved by generating a protective immune response using nonviable parasite antigens such as *T. parva* proteins or even peptides. Experiments indicate that killing of *T. parva* infected T-lymphocytes is mediated by cytotoxic T lymphocytes (CTLs) rather than immunoglobulins (antibodies) (Baldwin et al. 1988; McKeever 2001; Pearson et al. 1979). Generating a protective CTL response with a vaccine requires the identification of *T. parva* antigens able to induce the production of effector lymphocytes. This requires antigen processing and insertion of parasite proteins into both MHC class II and MHC class I molecules displayed at the cell surface. The MHC class I-peptide complex is recognized by effector CTL. The efficiency of MHC class I presentation of a parasite epitope depends on the cleavage pattern of the parent protein (Gromme and Neefjes 2002). Research has not yet fully unraveled the multiple protease activities and mechanisms associated with the generation of antigenic peptides for MHC class I presentation. The only conclusive method to distinguish antigenic parasite peptides with the potential to provoke a protective CTL response is to isolate them directly from MHC class I molecules.

Epitopes that are inserted into MHC molecules are derived from a pool of peptides representing the entire protein repertoire of the cell, including peptides generated from intracellular parasites. To identify the processed parasite peptides presented to CTLs by MHC class I molecules, theoretically one needs to elute them directly from the MHC molecules. As MHCs are membrane bound molecules, the relatively harsh techniques required to isolate them may result in the loss of their non-covalently associated peptides. It is known that peptides are loaded onto MHC class I molecules by a series of ER

resident chaperones. Isolation of the precursor peptides from these soluble chaperones would require gentler techniques that would retain the antigenic peptides destined for association with MHC class I molecules. Gp96, an endoplasmic reticulum heat shock protein (HSP) is one of these chaperones. Isolation of gp96-bound peptides from *T. parva* infected T-lymphocytes should liberate both host and parasite peptides. A mass spectrometry based comparison of gp96-eluted peptide profiles obtained from *T. parva* infected and uninfected cells could potentially identify antigenic parasite peptides. This thesis describes the development of methods that will allow identification of MHC class I-associated peptides from infectious intracellular pathogens, using *T. parva* as a model.

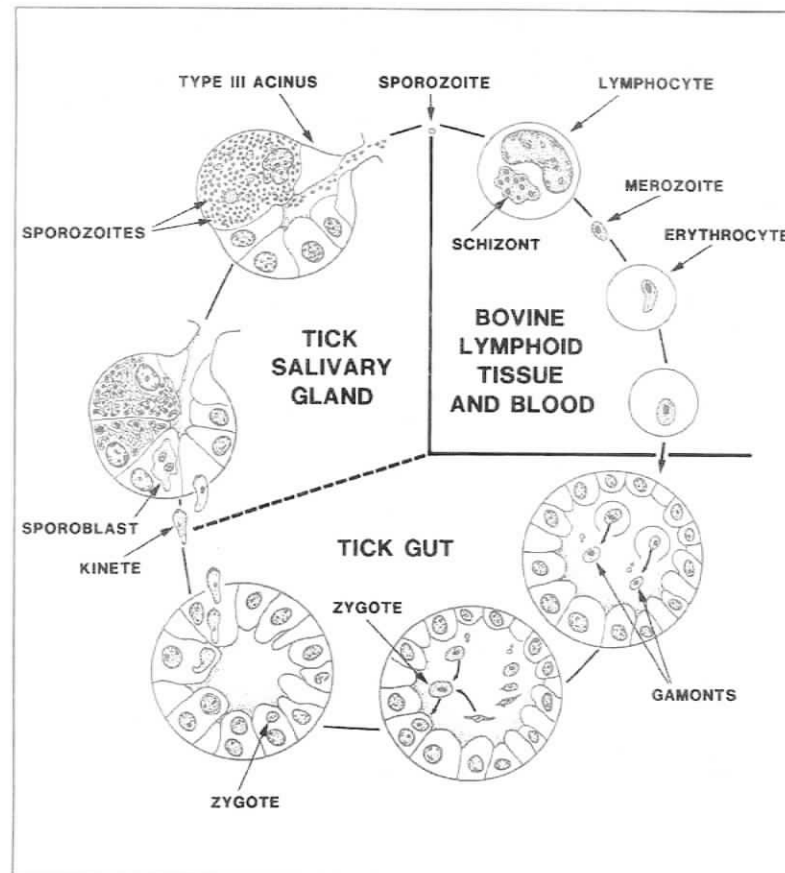
LIFE CYCLE OF *T. PARVA* IN BOTH VECTOR AND HOST

Theileria parva is the causative agent of three epidemiologically distinct diseases, East Coast fever (*T. p. parva*), Corridor disease (*T. p. lawrencei*) and January disease (*T. p. bovis*) (Uilenberg 1999). ECF, the most devastating of the three diseases, is present in 11 African countries while the tick vector, *R. appendiculatus*, is found in 15 countries. *R. appendiculatus* is a three-host tick, a life cycle classification considered to be evolutionarily primitive where the larva, nymph and adult feed on three separate hosts (Morzaria et al. 2000; Norval 1992). *R. appendiculatus* passes the ECF parasite transstadially, from one life cycle stage to another through a moult (Norval 1992). No known symbiotic relationship exists between *T. parva* and *R. appendiculatus*; the tick demonstrates reduced reproductive performance while harboring the parasite (Watt and Walker 2000).

The *T. parva* life cycle involves many morphologically distinct life cycle stages as the parasite cycles between the tick vector and mammalian host. When *R. appendiculatus* ingests a *T. parva*-infected bloodmeal, lysis of the erythrocytes liberates free piroplasms, the tick-infective stage of the parasite. In the tick gut the piroplasms develop into gametes and enter sporogony, an asexual lifecycle phase resulting in infective sporozoites that develop within E cells of the tick salivary glands (Norval 1992). Upon host attachment, 40,000 to 50,000 sporozoites per E cell are available for emission into the attachment lesion. Inflammation in reaction to tick feeding is thought to attract sporozoite target cells, the bovine T-lymphocytes. The severity of the induced disease is directly proportional to the dose of sporozoites inoculated by the feeding tick (Norval 1992).

While feeding, infected ticks inoculate susceptible livestock with sporozoites, the cattle-infective life cycle stage (McKeever 2001). The small, spherical sporozoites are non-motile and therefore their irreversible interaction with target host cells is a chance event (Shaw 2003). Once attached to the host cell surface, sporozoites quickly gain entrance through a endocytosis resulting in the sporozoites completely surrounded by host membrane (Shaw 2003). Once inside the cell the host membrane is shed leaving the sporozoite free in the cytoplasm (Shaw 2003). A host-derived microtubule system organizes around the intracellular sporozoite and 24-48 hours post infection the replicative form of the parasite develops, termed the schizont (Kaufmann 1996). The schizont is able to transform T-lymphocytes and is the only known eukaryote able to induce uncontrolled host cell proliferation, essentially cancer, in mammals (Heussler et

al. 2002). The rapid clonal expansion and metastasis results in dissemination of the parasitic infection to a variety of tissues (Honda et al. 1998). The multinucleated schizont form remains associated with the microtubule system and becomes entangled in the host cell spindle apparatus guaranteeing distribution to both daughter cells during mitosis and cytokinesis (Dobbelaere et al. 2000). Schizonts are capable of logarithmic growth resulting in a 10-fold increase in number over 72 hours (Association 1998a; Norval 1992). Survival of the parasite drives a small population of schizonts to enter a distinct morphological stage known as merozoites, which are liberated in an uninucleated form from the infected lymphocytes to infect erythrocytes. Within erythrocytes the merozoites develop into piroplasms, the infective stage for *R. appendiculatus*, thus completing the mammalian portion of the *T. parva* life cycle.



CELL MEDIATED IMMUNITY

Once attached to the host cell surface, sporozoites enter bovine T lymphocytes in less than 3 minutes, thus preventing the humoral immune response from efficiently clearing the parasite pathogen (Shaw 2003). A strong cell-mediated immune response is responsible for clearing the host of the predominantly intracellular *T. parva* parasites (Pearson et al. 1979). Most nucleated cells, including T-lymphocytes, are studded with MHC class I molecules on their surface. These polymorphic molecules contribute to the cell-mediated branch of the immune response by acting as molecular flags for effector cells. MHC class I molecules bind intracellularly processed (endogenous processing pathway) peptides and this peptide-MHC complex is recognized by CD8⁺ cytotoxic T-lymphocyte (CTL) effector cells. The collaboration between the local cytokine environment and successful binding of the CTL receptor with the antigenic peptide-MHC class I complex results in lysis of the peptide-bearing cell. Because MHC class I molecules are polymorphic they can bind a variety of peptides. The genotype of the bovine host defines the ability of MHC class I molecules to bind immunogenic *T. parva* peptides.

ANTIGEN PROCESSING

In eukaryotic cells the folding and loading of nascent MHC class I molecules with peptides occurs in the ER lumen by multiple chaperones yielding a stable complex destined for the cell surface. The ability to bind reversibly to a diverse array of peptides is a necessary component of ER chaperone function. In the relay of chaperones transporting peptides to be loaded onto MHC class I, gp96 is thought to be the last

acceptor prior to MHC loading (Srivastava et al. 1994). This coupled with the fact that gp96 is the most abundant chaperone in the ER lumen, implies that the gp96 population should carry all of the peptides generated for MHC class I association in that particular cell (Srivastava et al. 1994). It is postulated that the peptides chaperoned by gp96 are processed further before their final association with nascent MHC class I molecules yet it has been shown that the peptides isolated from gp96 in a virus infected cell were able to elicit a virus specific MHC class I restricted CTL response (Blachere et al. 1993). Therefore, it is not important whether the peptides are precursors or identical to those loaded onto MHC class I, as they are able to elicit an antigen specific CTL response, the same protective immune response needed to generate immunity to ECF.

It is relevant and important to identify *T. parva* schizont proteins that are processed by infected bovine host cells and presented to the cell-mediated immune system for identification by CTL effector cells. The work presented in this thesis describes the development of methods for ultimate use in identifying *T. parva* peptides involved in eliciting cell-mediated immune responses against parasite-infected bovine T cells. In this way, candidates for development of a vaccine may be identified.

CHAPTER 2. ENRICHMENT OF MOLECULES OF THE BOVINE ANTIGEN PROCESSING PATHWAY AND DERIVATION OF SPECIFIC MONOCLONAL ANTIBODIES.

INTRODUCTION

The MHC class I molecules play an essential role in immune surveillance as peptide binding transmembrane glycoproteins that decorate the exterior of most nucleated cells. Their function is to display endogenously synthesized protein fragments for scrutiny by effector CD8⁺ T lymphocytes of the cell-mediated immune system. This branch of the immune system in part protects against intracellular pathogens and is therefore instrumental in the detection and clearance of the intracellular pathogen *Theileria parva*. CD8⁺ T lymphocytes, via their specific T cell receptors (TCR) recognize the topographic arrangement of antigenic peptide complexed with host class I MHC molecules. The normal complement of MHC class I-associated antigenic peptides is derived from the degradation of cytosolic and nuclear proteins. When an intracellular organism infects a cell, pathogen proteins contribute peptides to the MHC class I-associated pool. Thus, cell surface display of these foreign peptides in association with MHC class I molecules allows CD8⁺ T lymphocyte-mediated recognition of cells harboring the intracellular pathogen. Recognition by CD8⁺ T lymphocytes results in target cell death, freeing the host of the intracellular infection. In this regard, the unique immunological identity of each cell is represented by the peptides associated with class I MHC molecules at the cell surface.

While the peptides intimately associated with MHC class I molecules represent the protein repertoire synthesized by the cell, they do not represent the entire precursor protein. The complex rules of antigen processing dictate that only defined portions of the parental protein, which satisfy specific binding parameters, will be associated with class I MHC molecules. Intriguingly, a wide variety of peptides are able to satisfy these properties. The promiscuity of the antigen-presenting molecules assures that peptides originating from most intracellular pathogens will be presented to the cell-mediated immune system. After processing, the peptides that successfully associate with class I MHC molecules are 8-10 amino acids in length with anchor residues located at both the N and C termini (Yewdell et al. 2003). These peptides are held in an extended conformation, tethered at both ends by the anchor residues, while arching away from the floor of the peptide binding cleft (Kuby 1997).

The selection of peptides able to satisfy the class I MHC binding characteristics is implemented on various levels. Candidate peptides are proteolytically generated in the cytosol by proteasomes. The peptides produced have an average length of 7 residues, thus many are too small for association with class I MHC (Yewdell et al. 2003). The heterodimeric protein called the transporter associated with antigen processing (TAP) preferentially translocates peptides of 8-13 residues into the lumen of the endoplasmic reticulum. Potential MHC- destined peptides are therefore lost due to over processing by the proteasome and selective transport into the ER lumen by TAP.

The peptides that successfully gain entrance into the ER lumen are protected by chaperones from nonspecific aggregation and premature degradation. There is evidence that one of the chaperones, gp96, participates in the antigen-processing pathway. Gp96 is among the most abundant components of the ER lumen and possesses similar multi-peptide-binding ability as class I MHC (Li et al. 2002; Blachere et al. 1997). The peptides associated with gp96 are able to induce antigen-specific, protective T-cell responses similar to those induced by MHC class I-peptide complexes (Heike et al. 1994; Udono et al. 1994; Blachere et al. 1993; Arnold et al. 1995). This can be explained by the fact that the peptides associated with gp96 are from the same ER pool of peptides optimized for binding and presentation by MHC class I molecules (Linderoth et al. 2001; Sastry and Linderoth 1999; Spee and Neefjes 1997).

In the absence of peptide, the MHC class I structure is very unstable. Within the ER lumen, newly synthesized class I MHC molecules sequentially interact with dedicated molecular chaperones prior to binding peptide (Pamer and Cresswell 1998). Calnexin is the first to bind and is successively replaced by the peptide-loading complex comprised of the MHC I accessory molecules calreticulin, TAP, tapasin and ERp57. A specialized enzyme, disulfide isomerase ERp57, catalyzes the formation of disulfide bonds to generate a mature, peptide-accepting MHC class I molecule (Paulsson and Wang 2003). Within the peptide-loading complex, tapasin facilitates association with TAP and subsequent transfer of the peptide from TAP to the class I MHC complex (Paquet and Williams 2002). Upon loading of peptide into the MHC class I antigen-binding groove,

the complex is released from all auxiliary molecules and is then transported via the Golgi body to the cell surface (Chirmule 2004).

To obtain MHC-destined peptides my strategy was first to isolate bovine gp96 molecules using affinity chromatography and physiological conditions that favor peptide retention. This approach necessitates the initial production of gp96 specific monoclonal antibodies for the affinity matrix.

MATERIALS AND METHODS

2.1 Preparation of bovine liver glycoproteins for derivation of monoclonal antibodies.

To develop and optimize a method for isolation of gp96, bovine liver, an abundant tissue, was used. Bovine liver tissue was obtained fresh from a slaughterhouse (Schmidt's Meats, Duncan, BC), placed on ice for transport to the University of Victoria and there cut into 30 g portions and frozen at -80 °C until use. For each isolation performed, a single 30 g portion was thawed in 60 mL distilled water containing a protease inhibitor cocktail (Protease Inhibitor Cocktail Set V, EDTA-Free, Calbiochem, La Jolla, CA). The thawed material was homogenized on ice (24,000 rpm) using an electric tissue homogenizer (Disperser DIAX 600; Heidolph Elektro GmbH & Co KG, Kelheim, DRG). The homogenate was centrifuged at 5000 x g for 30 min at 4 °C to remove debris and the supernatant was ultracentrifuged at 100,000 x g for 90 min at 4 °C to obtain soluble molecules. The soluble supernatant proteins were precipitated by adding ammonium sulfate to 50 % then 70 % saturation at 4 °C. After 12 hours the mixture was centrifuged at 14,100 x g for 20 min at 4 °C and the supernatant was removed by pipetting. Excess supernatant was removed from the pellet by inversion of the tubes for 30 min. The pellets (precipitates) were solubilized in Con A-binding buffer (20 mM Tris-HCl, 0.5 M NaCl pH 7.4) and loaded onto a 13.5 cm³ column of Con A Sepharose™ (Amersham Biosciences Inc, Baie d'Urfé, PQ). The column had been equilibrated previously by washing with 6 column volumes of Con A-binding buffer. The sample was recirculated over the column at 4 °C overnight at 0.9 mL/min using a Gilson peristaltic pump (Gilson Minipuls 2; Mandel Scientific Company Inc, Guelph, ON). The column was washed

with 10 column volumes of Con A-binding buffer over 2.5 hours and the eluate was monitored until the OD₂₈₀ was less than 0.02. Bound proteins were eluted by application of one third column volume of elution buffer (0.5 M methyl alpha-D mannopyranoside in Con A-binding buffer) followed by incubation of the entire column at 37 °C for 30 min before 15 x 5 mL fractions were collected and assessed for protein concentration by determining the OD₂₈₀. Fractions with an OD₂₈₀ above 0.2 were pooled (20 –25 mL) and protease inhibitor cocktail added prior to volume reduction to < 50 % by lyophilization. One mL of the concentrated pool was loaded onto a C₈ high performance liquid chromatography (HPLC) column (Brownlee Aquapore RP-300; PerkinElmer Canada Inc., Woodbridge, ON) and the glycoproteins separated further using a 2 – 98 % gradient of 0.075 % trifluoroacetic acid in acetonitrile (buffer B) over 10 minutes, and the eluate was monitored by OD₂₃₀. The protein peaks eluting at 65 – 98 % buffer B were pooled, the acetonitrile removed using a Speed Vac Concentrator (Savant, Hicksville, NY), and the protein content determined by OD₂₈₀ (an assumption that 1 OD₂₈₀ = 1 mg protein). This glycoprotein-enriched sample was first characterized by gel electrophoresis and then used as the immunogen for derivation of monoclonal antibodies.

2.2 One-dimensional gel electrophoresis.

Twenty seven µL of the glycoconjugate immunogen preparation were loaded onto pre-cast NuPAGE 4-12% Bis-Tris 1.0 mm X 12 well gels (Invitrogen, Carlsbad, CA) for protein analysis by one dimensional sodium dodecyl sulfate polyacrylamide gel electrophoresis (1-D SDS-PAGE). The gels were run on a Novex Mini-Cell apparatus (Invitrogen, Carlsbad, CA) using NuPAGE MES SDS running buffer (50 mM MES, 50

mM Tris Base, 3.47 mM SDS, 1.03 mM EDTA) in both the inner and outer reservoir with an additional 0.25% (v/v) NuPAGE Antioxidant (proprietary) added to the inner reservoir. Proteins were separated by electrophoresis at 200 V for 35 min. A 10-180 kDa prestained molecular mass ladder (8 μ L; #0801; MBI Fermentas, Burlington, ON) was run on each gel. Following electrophoresis, gels were either stained with colloidal Coomassie Brilliant Blue G-250 or the proteins were electrophoretically transferred onto membranes for subsequent immunoblot analysis.

2.3 Two-dimensional gel electrophoresis.

High-resolution two-dimensional sodium dodecyl sulphate polyacrylamide gel electrophoresis (2-D SDS-PAGE) was performed using the ISO-DALT multiple 2-D gel system (Beecroft et al. 1993; Tolson et al. 1989). Immunogen preparation (300-500 μ L) was concentrated using a Speed Vac Concentrator (Savant, Hicksville, NY) to near dryness and the concentrated material solubilized in 35 μ L of urea sample buffer (9 M urea, 4 % NP-40 (v/v), 2 % Invitrogen pH 9-11 ampholines (v/v), 2 % DTT (w/v)). Samples were centrifuged for 30 sec at 10,000 x g to remove insoluble material and the supernatants were loaded onto pre-focused tube gels containing pH range 3-10 ampholines (Pharmalyte 3-10, Amersham Pharmacia, Upsala, Sweden). First dimension isoelectric focusing was conducted at 800 V for 18 h (14,400 Vh). Following electrophoresis, the tube gels were equilibrated for 15 min at room temperature in equilibration buffer and immediately mounted onto 5-15 % gradient SDS-PAGE slab gels with the acidic end positioned to the left. Electrophoresis was performed at 4 $^{\circ}$ C at 1 Amp until the dye front was 1 cm from the bottom of the gel (approximately 5 hours).

After electrophoresis the gels were fixed and stained with colloidal Coomassie Brilliant Blue G-250.

2.4 Staining of proteins with colloidal Coomassie Brilliant Blue G-250.

Gels were agitated gently in fixative (50 % (v/v) ethanol, 3 % (v/v) ortho phosphoric acid) for 18 hours at room temperature, washed three times for 30 min in distilled water and allowed to equilibrate in Neuhoff's solution (16 % (w/v) ammonium sulphate, 25 % (v/v) methanol, 5 % (v/v) ortho phosphoric acid) (Neuhoff et al. 1988) for one hour with gentle agitation. One gram of Coomassie Brilliant Blue G-250 (EM Science, Gibbstown, NJ) was sprinkled into the Neuhoff's solution and staining was performed with continuous shaking for 3-5 days. Once well-stained protein spots were visible, gels were either scanned and protein spots cored (for mass spectrometry) or the intact gels were transferred into a 20 % (w/v) ammonium sulphate solution for storage at 4 °C (Neuhoff et al. 1988). Digital images of both 1-D and 2-D stained gels were captured by scanning of wet gels at 300 dpi using a colour scanner (UMAX Astra 3400, Fremont, CA) after briefly rinsing the gels in distilled water. The images were manipulated and stored as JPEG and/or TIFF files using Photoshop 7.0 graphic software (Adobe Systems Inc., San Jose, CA).

2.5 Derivation of monoclonal antibodies.

Two female BALB/c mice (6 - 8 weeks old) were immunized with the glycoconjugate immunogen mixture. Each mouse received five intraperitoneal injections of 25 µg of the immunogen preparation in 0.2 mL of PBS. The first injection was administered in complete Freund's adjuvant and, over a three-month period, four subsequent injections were given in incomplete Freund's adjuvant (Invitrogen, Burlington, ON). Seven days after the final injection, both mice were test bled from the lateral saphenous vein using a 26-gauge needle and heparinized capillary tubes (Chase Scientific Glass Inc, Rockwood, TN). From each mouse, 25 µL of blood was collected. The blood was diluted 1/25 with PBS, centrifuged at 16,000 x g for 5 min to remove cells and the cell-free plasma dilution was titrated by ELISA. Although the antibody titres were judged to be satisfactory, a decision was made to try both *in vitro* and *in vivo* boosting procedures prior to cell fusion.

In vitro boosting of murine B-lymphocytes was performed as described by Robert Beecroft (ImmunoPrecise Antibodies Ltd.). Briefly, three weeks after the last injection, one mouse was CO₂ anesthetized and the blood collected by cardiac bleed using a 1 mL syringe fitted with a 27-gauge needle. The spleen was aseptically removed and the lymphocytes purified using Ficoll-Paque (Amersham Biosciences Inc, Baie d'Urfé, PQ) according to the manufacturer's instructions. The washed, purified lymphocytes were cultured in 6 well tissue culture plates (Becton Dickinson, Franklin Lakes, NJ) in medium containing 20 % (v/v) conditioned medium (supernatant from EL4 thymoma cells stimulated with phorbol myristic acetate; (Ma 1984)). Immunogen was added (75 µg per

mL) and the lymphocyte cultures were incubated for 3 days at 37 °C in a 5 % CO₂ in air mixture. The stimulated murine lymphocytes were then pooled and fused with SP2/0 parental myeloma cells at a 5:1 ratio. Single step selection and cloning of hybridomas was performed using the ClonaCell-HY™ system (StemCell Technologies Inc., Vancouver, BC) following the instructions of the manufacturer. Essentially the cell fusion mixture was diluted and plated in a semi-solid methylcellulose medium containing hypoxanthine, aminopterin and thymidine (HAT) and B-cell growth factors, allowing single-step selection and cloning of the hybridomas.

The second mouse was boosted with two additional intraperitoneal injections of 15 µg of immunogen in incomplete Freund's adjuvant over a four week period followed by an intravenous (tail vein) injection of 15 µg immunogen in 50 µL sterile saline. Three days after the last injection, the spleen was removed, a single cell suspension was made and the lymphocytes were purified using Ficoll-Paque. Finally, the lymphocytes were fused and the hybridomas were selected and cloned as described above.

After isolation and growth of individual hybridoma clones, tissue culture supernatants were first screened by indirect ELISA on both the immunogen preparation and on human transferrin. Hybridoma clones that tested positive on immunogen and negative on human transferrin were analyzed further using a variety of techniques to characterize the monoclonal immunoglobulins and their respective antigens.

2.6 Enzyme-linked immunosorbent assay.

Hybridoma supernatants were first screened in indirect ELISA (Tolson et al. 1989) using the immunogen preparation as solid-phase antigen. ELISA plates (Falcon 3915 PRO-BIND™ Assay Plates, Becton-Dickinson, Oxnard, CA) were coated with 5 µg per well of the immunogen mixture in distilled water and dried overnight at 37 °C. Control plates were coated with a 1 µg solution of human transferrin in PBS. Screening of hybridoma supernatants was performed on human transferrin to detect non-specific antibodies.

Undiluted hybridoma tissue culture supernatants were used as the primary antibodies and a 1:2000 dilution of alkaline phosphatase conjugated goat anti-mouse IgG/IgM (Cedarlane Laboratories, Hornby, ON) was used as the secondary antibody. After initial screening, antibodies in tissue culture supernatants from selected hybridomas were isotyped using an antigen-capture ELISA kit (American Qualex, La Mirada, CA) according to instructions supplied by the manufacturer.

2.7 Immunoblotting.

Immunoblotting using BioTrace™ polyvinylidene difluoride (PVDF) membrane (Pall Corporation, Ann Arbor, MI) was performed essentially as previously described (Beecroft et al. 1993) with the exception that an increased transfer time (to 45 min) and a more sensitive substrate (SuperSignal West Dura chemiluminescence substrate; Pierce Chemical Company, Rockford, IL) were used. A 1:1,000 dilution of a positive control antibody (rat anti-Grp94; SPA-850, Stressgen Biotechnologies, Victoria, BC) and 1:2 dilutions of hybridoma tissue culture supernatants were used as primary antibodies while a 1:50,000 dilution of secondary antibody (goat anti-rat IgG-horseradish peroxidase

conjugate; Cedarlane Laboratories Ltd., Hornby, ON) was employed. Kodak Biomax MR film (Eastman Kodak Company, Rochester, NY) was used to detect chemiluminescence. After development of the autoluminograms, proteins were stained on the PVDF membrane with GelCode[®] Blue (Pierce Chemical, Rockford, IL). The exposed film was superimposed on the stained PVDF membrane to reveal the precise location of the immunoreactive protein bands in relationship to the entire protein profile.

2.8 Dot blotting.

Dot blots were performed using nitrocellulose membrane (BioTrace[®] NT Pure nitrocellulose blotting membrane; Pall Corporation, Ann Arbor, MI). Immunogen preparations (5.0 and 2.5 μg) and human transferrin (1.0 μg) were spotted in 5 μL volumes and dried down at room temperature. The antigen spotted membrane portions (2.5 cm x 1 cm) were processed individually in 1.5 mL microcentrifuge tubes. Immunodevelopment was performed as described for immunoblotting (see above). To ensure removal of unbound antibodies, large Petri dishes and large volumes of wash buffer were employed for washing after primary and secondary antibody application and incubation.

2.9 Sample preparation for mass spectrometry.

Protein samples were prepared for mass spectrometric analysis of tryptic peptides as described previously (Haddow et al. 2002). Briefly, colloidal Coomassie Brilliant Blue G-250 stained protein spots were cored from 2-D gels using 4 mm plastic straws and the gel plugs were transferred to 1.5 mL Maxymum Recovery microcentrifuge tubes

(Axygen Scientific, Union City, CA) containing 200 μL of 20 % (v/v) acetonitrile and 1 M ammonium bicarbonate. The straws and tubes were previously rinsed with 95 % HPLC grade ethanol to remove any contaminants. The excised spots were de-stained over two days in several washes of 50 % (v/v) methanol/ 5 % (v/v) acetic acid, dehydrated with acetonitrile, reduced for 30 min with 50 mM dithiothreitol at 56 °C and alkylated for 30 min with 100 mM iodoacetamide at 45 °C. The carboxyamidomethylated protein spots were dehydrated with acetonitrile and rehydrated with 100 mM ammonium bicarbonate before being digested overnight at 37 °C with 30 μL of 20 ng/ μL sequencing grade, modified porcine trypsin according to the manufacturer's directions (Promega, Madison, WI). Peptides were extracted from the gel using three 10 μL elutions with 10 % (v/v) formic acid. The resulting eluate pool was reduced to a final volume of 20 μL in 500 μL Maxymum Recovery microcentrifuge tubes (Axygen Scientific, Union City, CA) and processed for mass spectrometry.

2.10 MALDI-TOF mass spectrometry.

Peptides from each trypsin-digested sample were desalted and concentrated using a ZipTip (C_{18} resin; P10, Millipore Corporation, Bedford, MA). For each sample, 1.0 μL of the desalted peptide mixture was mixed (1:1) with the matrix alpha-cyano-4-hydroxycinnamic acid (10 mg/mL in 50 % acetonitrile/0.1 % TFA, Sigma Chemical Co. St. Louis, MO) spiked with 1 femtomole each of internal standards (bradykinin, fragment 2-9 FW 904.4681 and adrenocorticotrophic hormone, fragment 18-39 FW 2465.1989; Sigma Chemical Co. St. Louis, MO) and spotted onto a Voyager, 100 position, stainless steel MALDI plate (Applied Biosystems, Foster City, CA). An Applied Biosystems

Voyager DE-STR mass spectrometer (Applied Biosystems, Foster City, CA) running in delayed extraction, reflectron mode was used to acquire MALDI-TOF data. Selected peptide masses were submitted to MS-Fit (Protein Prospector software package; San Francisco, CA: <http://prospector.ucsf.edu/>) and Mascot (Matrix Science, London, UK: <http://www.matrixscience.com/>) for database searching and determination of peptide mass maps.

RESULTS

A) ENRICHMENT OF GLYCOPROTEINS FROM BOVINE LIVER CELLS

Glycoproteins from the homogenate and ammonium sulfate fractionated bovine liver samples were separated by 1-D gel electrophoresis and stained with colloidal Coomassie Brilliant Blue G-250 (Figure 2.1).

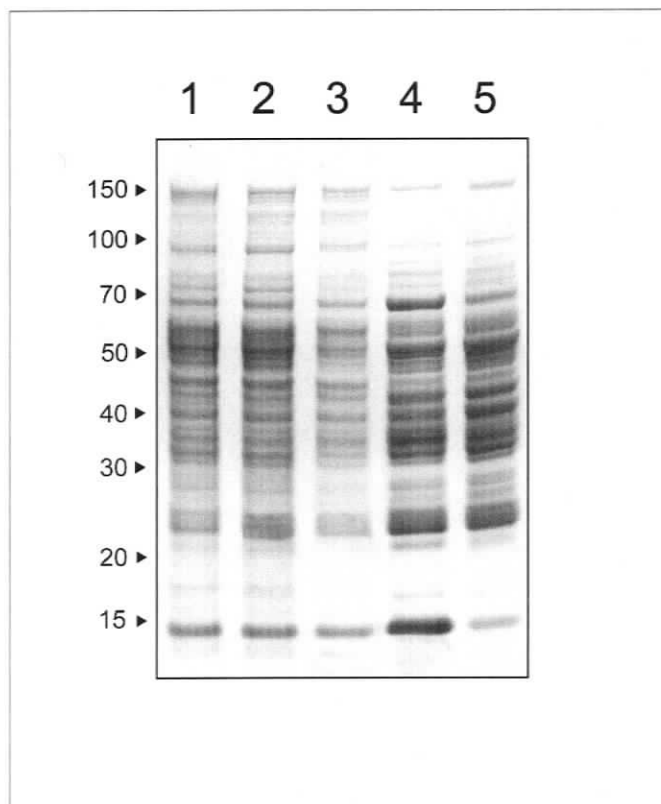


Figure 2.1 *SDS-PAGE of homogenate and ammonium sulfate fractionated bovine liver tissue.*

Solubilized bovine liver proteins were separated on a pre-cast 4-12% Bis/Tris 12 well gel (Invitrogen). Lane 1, liver homogenate; lane 2, 5000 x g centrifuge supernatant; lane 3, 100,000 x g ultracentrifuge supernatant; lane 4, 50 % ammonium sulfate cut and lane 5, 70 % ammonium sulfate cut. Proteins were stained using colloidal Coomassie Brilliant Blue G-250. Positions of molecular masses (kDa) are depicted with arrowheads on the left side of the gel.

Only slight differences between the crude tissue homogenate and the clarified sample were seen (lanes 1 and 2). The protein banding pattern of the supernatant from the ultracentrifuged sample indicates that most of the proteins were soluble (lane 3). Minimal differences between the 50 % and 70 % ammonium sulfate precipitations were observed (lanes 4 and 5). Due to the high degree of protease activity usually found within liver tissue, the slight reduction in the number of high molecular mass protein bands and a corresponding augmentation of mid mass proteins after the precipitation process may be the result of degradation, despite the use of protease inhibitors during the solubilization/fractionation procedure. Major protein bands prominent throughout the fractionation process were observed at 67, 55, 25 and 15 kDa.

Isolation of glycoproteins from the fractionated bovine liver sample was performed using Con A affinity chromatography. The glycoproteins were eluted from the Con A resin isocratically using 10 % methyl alpha-D mannopyranoside. The proteins in the eluted fractions were monitored by OD_{280} determination as seen in the elution profile, shown in Figure 2.2.

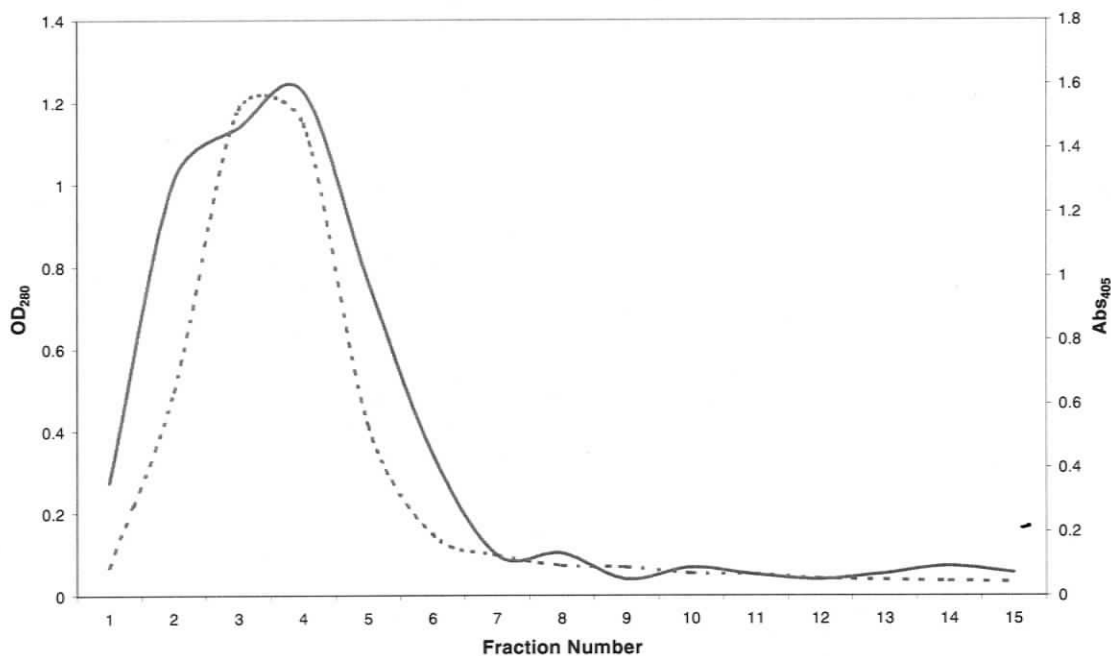


Figure 2.2 *Profile of bovine liver glycoproteins eluted isocratically from a Con A affinity column.*

Fractions (5 mL) eluted from a Con A affinity column were tested for their protein content by OD₂₈₀ (solid line) and gp96 content by indirect ELISA (dashed line).

A single broad glycoprotein peak was detected early in the elution process (Figure 2.2). Indirect ELISA performed on each fraction using a mAb specific for gp96 (Figure 2.2) showed that gp96 eluted from the column in a relatively tight peak comprised of fractions 2-5. To further analyze those fractions containing gp96, the proteins eluted from the Con A affinity column were separated by 1-D gel electrophoresis and transferred onto PVDF membrane before probing the membrane with an anti-gp96 monoclonal antibody (Figure 2.3). The gp96 containing fractions were pooled for further fractionation by reversed phase HPLC.

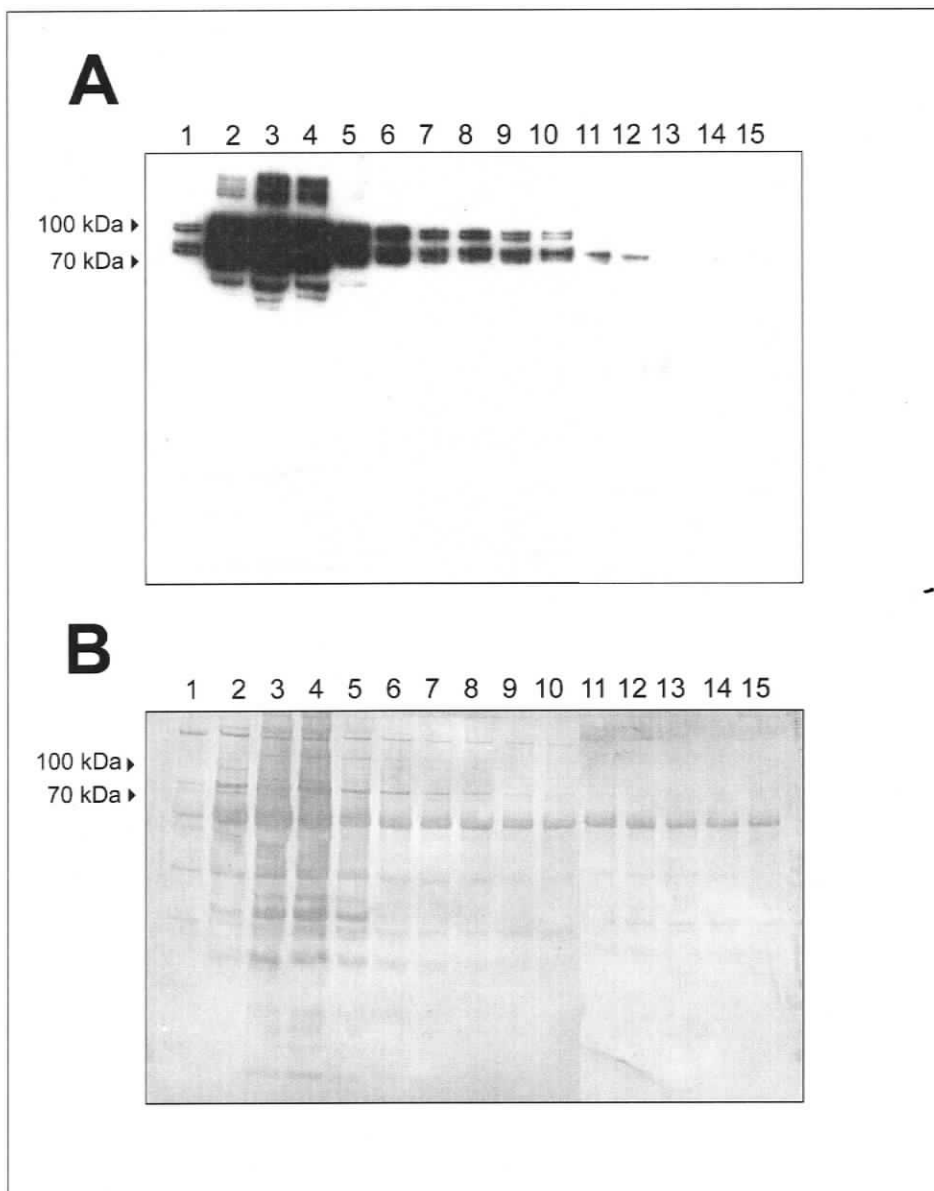


Figure 2.3 *Immunoblot analysis of glycoprotein fractions from Con A affinity chromatographic separation of bovine liver proteins.*

Proteins were separated using a pre-cast 4-12 % Bis/Tris 12 well gel (Invitrogen), electrophoretically transferred onto PVDF membrane and probed with anti-gp96 monoclonal antibody (Stressgen). Panel A, autoluminogram pattern of chaperone gp96 eluting from Con A affinity column. Panel B, colloidal Coomassie Brilliant Blue G-250 stained PVDF membrane of resolved glycoprotein fractions.

The gp96-specific mAb detected two distinct sets of double bands that ran between 70 kDa and 100 kDa (Panel A). In addition to these predominant doublets, the anti-gp96 mAb also recognized higher and lower molecular mass bands in the most concentrated fractions (2-4). The darkest bands and presumably the highest concentration of gp96 were observed in fractions 2-5, validating the ELISA results (Figure 2.2).

To assess the complexity of the fractions eluting from the Con A affinity column, the PVDF membrane was stained with GelCode Blue to visualize the number and relative abundance of the fractionated glycoproteins (Figure 2.3, Panel B). It is clear that there was a reduction in the number of resolved protein bands after Con A-enrichment compared with the colloidal Coomassie Blue stained gel of the ammonium sulfate precipitated bovine liver tissue (starting material) loaded onto the Con A affinity column shown in Figure 2.1, lane 5. Augmentation of two major glycoproteins (approximately 50 kDa and 90 kDa) was seen throughout the elution series.

Reversed phase HPLC (RP-HPLC) was used to remove the methyl alpha-D mannopyranoside Con A chromatography elution buffer from the pooled gp96-containing sample (Figure 2.4).

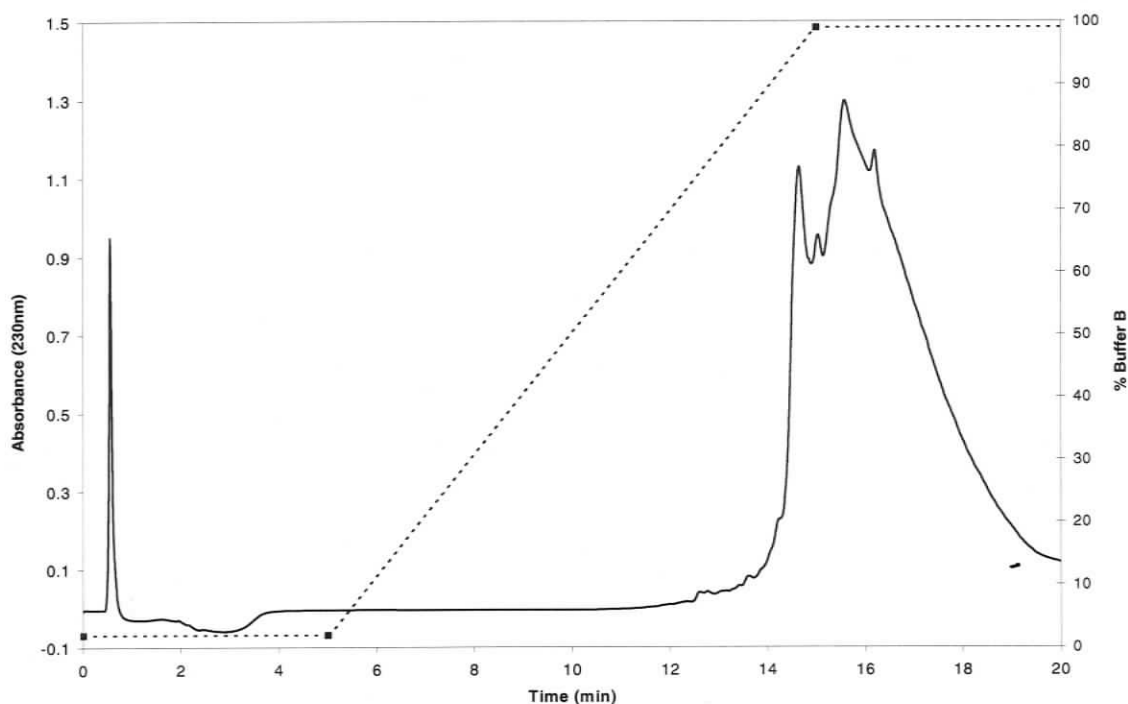


Figure 2.4 *RP-HPLC elution trace of molecules from Con A isolated bovine liver glycoproteins.*

Chromatogram of reversed phase HPLC separation of molecules from Con A purified bovine liver glycoproteins using a Perkin Elmer Brownlee Aquapore RP-300 column. A gradient of 2% - 98% B in 10 minutes with a flow rate of 0.5 mL/min was utilized. Mobile phase A: 0.1% TFA, mobile phase B: 0.075% TFA in acetonitrile. HPLC separation profile, solid line; buffer B gradient, dashed line.

Elution with a steep acetonitrile gradient resulted in the immediate removal of methyl alpha-D mannopyranoside and subsequent elution of the entire glycoprotein series.

Optimally, the gp96 glycoprotein was to be isolated with high purity, as it would be used as immunogen for the production of anti-gp96 monoclonal antibodies. Therefore, to purify gp96 from other contaminating glycoproteins present after affinity chromatography, HPLC separation using a less steep acetonitrile gradient was performed.

Multiple distinct peaks were detected at OD₂₃₀, but immunoblotting with the anti-gp96 mAb confirmed that all the peaks contained gp96 (data not shown). To reduce sample loss, it was decided that HPLC was to be used only to remove the methyl alpha-D mannopyranoside. The multiple glycoprotein peaks eluting from the C8 column between 14-18 minutes were pooled and the organic phase removed using a Speed Vac concentrator.

To determine the complexity of the final immunogen preparation to be used for production of mAbs, the glycoproteins in the pooled Con A-column eluate were separated by high-resolution 2-D gel electrophoresis. A representative 2-D gel electropherogram showing bovine glycoproteins stained with colloidal Coomassie Brilliant Blue G-250 is shown in Figure 2.5.

The multiple strongly stained protein spots visible on the 2-D gel confirmed the complexity of the immunogen mixture. As expected, many spots were aligned horizontally, a pattern characteristic of charge-shifted glycoproteins. Several darkly stained spots from different areas of the gel were cored for preparation of tryptic peptides and peptide mass mapping analysis by MALDI-TOF mass spectrometry (Table 2.1).

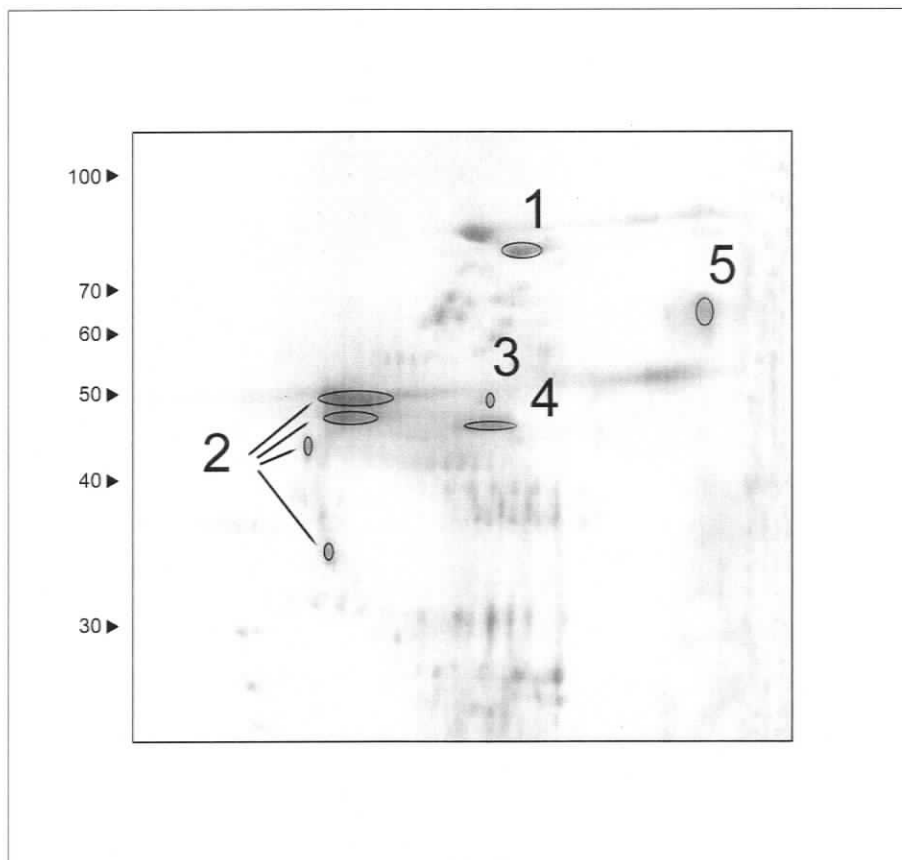


Figure 2.5 *Two-dimensional polyacrylamide gel analysis of fractionated glycoproteins from bovine liver tissue.*

The glycoproteins were stained with colloidal Coomassie Brilliant Blue G-250. The gel is oriented with the acidic end at the left with molecular masses (kDa) shown on the left side of the gel. First dimension isoelectric focusing utilized wide pH range ampholines (pH 3-10) and the second dimension molecular mass separation was performed using a 5-15 % gradient gel. Spot numbers correlate to the spots identified and described in Table 2.1.

Table 2.1 *Mass spectrometric identification (mass mapping) of bovine liver glycoproteins resolved by two dimensional gel electrophoresis.*

Protein spot	Molecular Mass ^a	pI ^b	Protein identity and Accession number ^c	Protein sequence coverage (%) ^d
1	92 654	4.76	<i>Bos taurus</i> glucose-regulated protein GRP94 precursor (BAB69766)	22%
2	46 524	4.31	<i>Bos taurus</i> calreticulin (S43376)	36%
3	72 185	5.03	DnaK-type molecular chaperone homologue (A29821)	21%
4	55 591	4.71	<i>Bos taurus</i> protein disulphide isomerase (E971018)	28%
5	79 870	6.75	<i>Bos taurus</i> transferrin (AAA96735)	9%

a) Calculated from the translated protein sequence.

b) Calculated from the translated protein sequence.

c) Protein identified using both Matrix Science (Mascot) and ProteinProspector (MS-Fit) databases. Accession number from NCBI.

D) Percentage of the protein sequence covered by matching of peptide masses to the parent sequence.

B) DERIVATION OF MONOCLONAL ANTIBODIES TO ENRICHED BOVINE LIVER GLYCOPROTEINS

After four immunizations with the bovine liver glycoprotein mixture obtained by Con A chromatography, sera were obtained after lateral saphenous vein bleeding of the mice. The sera were titrated by ELISA against the immunization mixture as solid-phase antigen. The antibody titration results are shown in Figure 2.6.

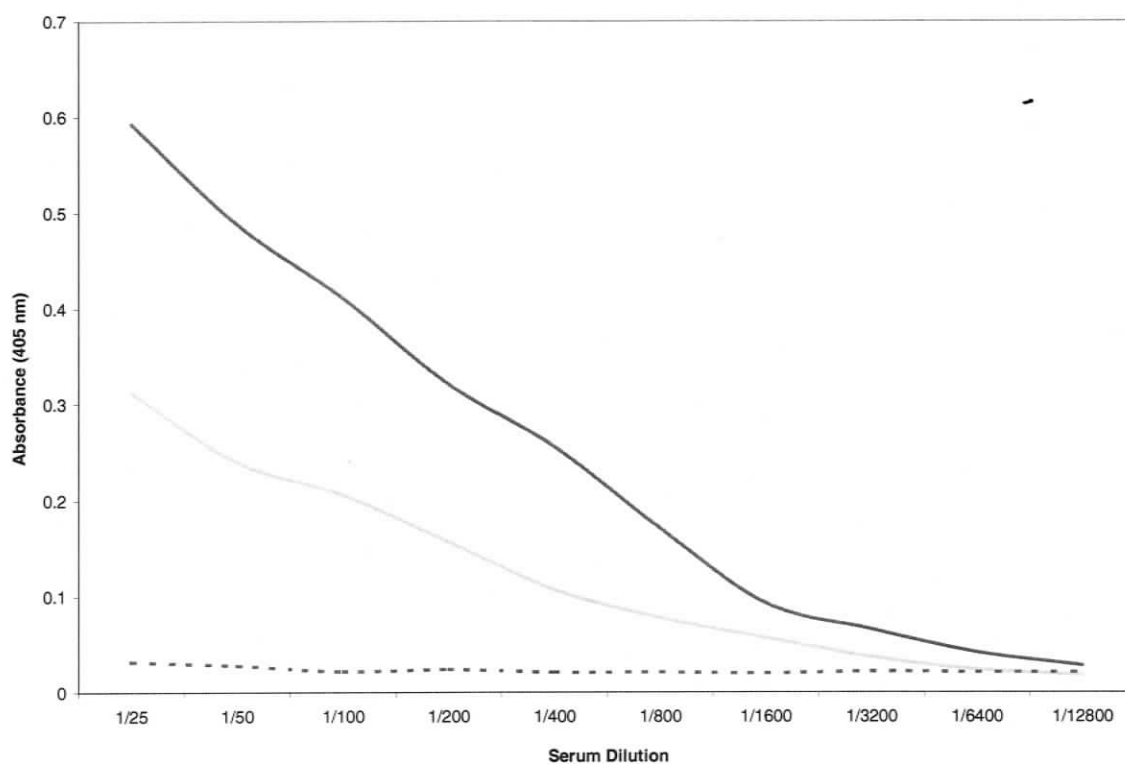


Figure 2.6 *ELISA titration of mouse antisera raised against bovine liver glycoproteins prior to in vitro stimulation of lymphocytes and cell fusion.*

Sera obtained from two female BALB/c mice after four immunizations were titrated against the glycoprotein immunization mixture. Mouse 1, black line; mouse 2, grey line; normal (prebleed) BALB/c mouse serum (control), dashed line.

Mouse number one produced antibodies that appeared to bind more strongly and was therefore used for the initial cell fusion after *in vitro* antigen stimulation. Interestingly, the titre (50 % of maximum binding) was 1/200 for each mouse.

Mouse number two was used after *in vivo* boosting. One mouse spleen was used for each fusion technique. From the initial fusion (*in vitro* boosting), more than 1000 hybridoma clones were generated and 672 of these were picked for culturing and characterization of their secreted antibodies. An initial ELISA screen using the glycoprotein mixture and purified human transferrin as the target antigens eliminated 633 hybridomas secreting nonspecific antibodies or non-secreting clones. Dot blotting of the remaining 39 hybridoma supernatants was performed as a prelude to immunoblotting (Figure 2.7).

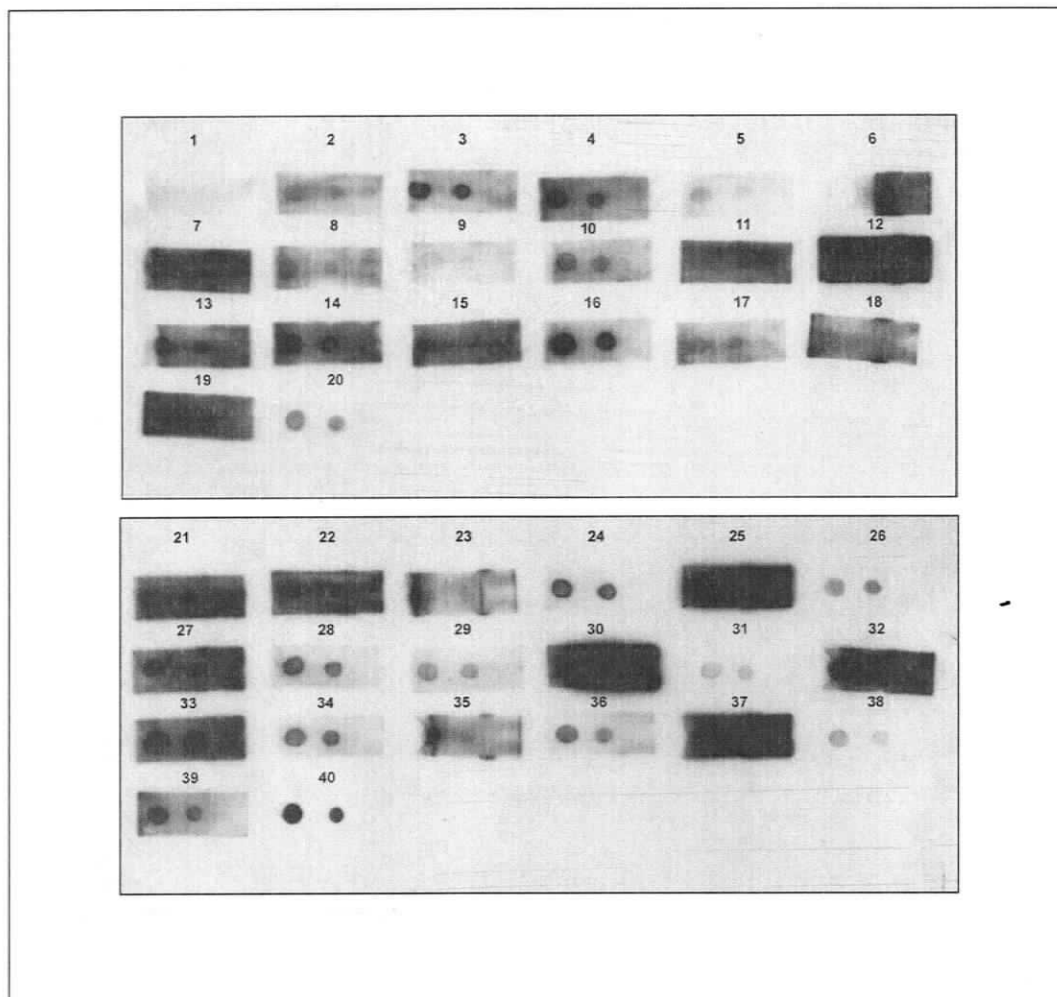


Figure 2.7 *Dot blot analysis of monoclonal antibodies raised against bovine liver glycoproteins (hybridomas derived after in vitro antigen stimulation).*

Dot blots were performed with tissue culture supernatants on two dilutions (5.0 and 2.5 μ g) of the glycoprotein immunogen mixture and 1.0 μ g human transferrin for a total of 3 spots/membrane piece. The numbers correspond to the hybridoma supernatant used as primary antibody.

1. 1A1	11. 3C1	21. 4B10	31. 5D10
2. 1A9	12. 3C6	22. 4B12	32. 5F9
3. 1B12	13. 3C7	23. 4C4	33. 5G5
4. 1C10	14. 3C10	24. 4D1	34. 6B6
5. 2B10	15. 3D9	25. 4D12	35. 6C5
6. 2D5	16. 3E5	26. 4F10	36. 6E1
7. 2F5	17. 3F5	27. 4H11	37. 7A1
8. 3A2	18. 3F7	28. 5A2	38. 7B2
9. 3B4	19. 3F11	29. 5A11	39. 7H2
10. 3B12	20. 4A7	30. 5D7	40. anti-gp96 (+ ctrl)

All 39 clones were found to be positive on native antigen by dot blot analysis thus they were further characterized by immunoblotting on denatured immunogen (ie. After SDS-PAGE separation) (Figure 2.8).

Of the 39 hybridoma clones tested, 31 secreted antibodies that reacted in immunoblots. Three distinct protein banding patterns were seen: a 53 kDa band, a 80 kDa band, or a composite of both. Some mAbs appeared to bind to a wide range of protein bands and their non-specificity for antigen was consistent with the dot blot results (Figure 2.7).

For the second fusion (*in vivo* boosting), the remaining mouse was immunized a total of six times with the glycoprotein mixture, the last time with an intravenous injection. Again an indirect ELISA was performed to measure the final serum antibody titre. The results are shown in Figure 2.9.

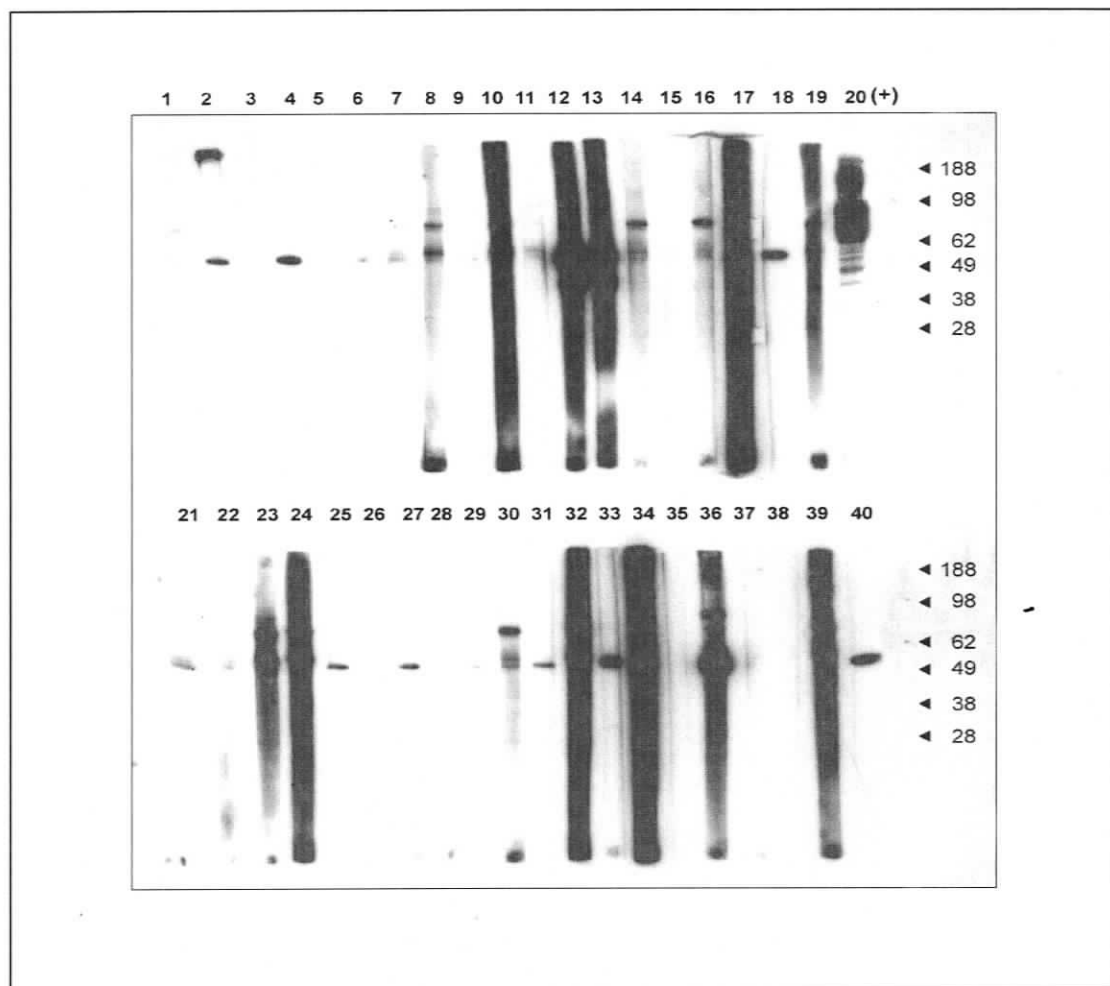


Figure 2.8 *Immunoblot analysis of monoclonal antibodies.*

Glycoproteins from the immunogen mixture were separated using a pre-cast, mono-well, 4-12% Bis-Tris gradient gel, blotted onto PVDF membrane, cut into 3 mm slices and probed with tissue culture supernatants from hybridomas derived using the *in vitro* immunogen boost fusion technique. Molecular masses (kDa) are shown on the right side of the figure. Numbers correspond to the hybridoma supernatant used as primary antibody.

1. 4B10	11. 5D10	21. 1A1	31. 3C1
2. 4B12	12. 5F9	22. 1A9	32. 3C6
3. 4C4	13. 5G5	23. 1B12	33. 3C7
4. 4D1	14. 6B6	24. 1C10	34. 3C10
5. 4D12	15. 6C5	25. 2B10	35. 3D9
6. 4F10	16. 6E1	26. 2D5	36. 3E5
7. 4H11	17. 7A1	27. 2F5	37. 3F5
8. 5A2	18. 7B4	28. 3A2	38. 3F7
9. 5A11	19. 7H2	29. 3B4	39. 3F11
10. 5D7	20. anti-gp96	30. 3B12	40. 4A7

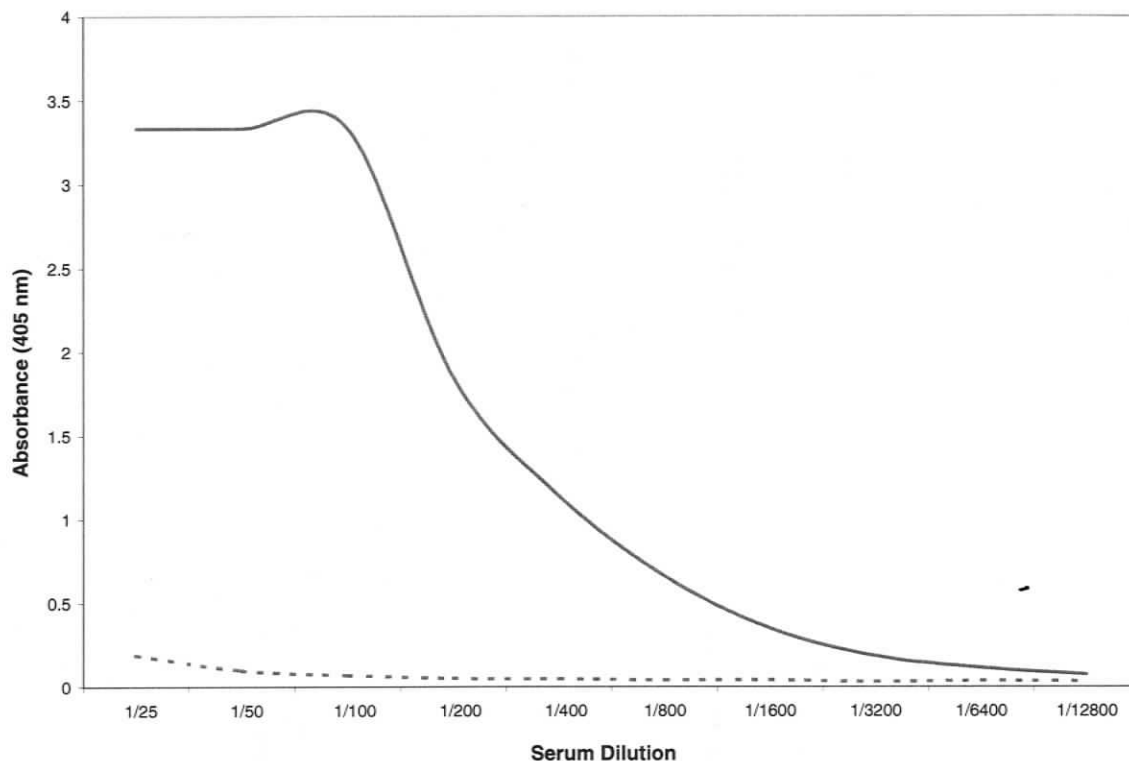


Figure 2.9 *ELISA titration of mouse antiserum raised against bovine liver glycoproteins prior to in vivo antigen stimulation of lymphocytes and cell fusion.*

Serum obtained from the remaining BALB/c mouse after six immunizations was titrated against the immunogen mixture. Test bleed serum, solid line; normal BALB/c mouse serum, dashed line.

The antibody titre was again found to be 1/200 with a maximum active dilution of 1/1600. While the titre did not increase after the additional two booster injections, the curve was indicative of a typical antibody titration ELISA result.

The second fusion also produced more than 1000 clones, 672 of which were picked for culturing and characterization. Thirty-eight of these hybridoma clones secreted antibodies specific for a component in the immunizing mixture and 21 of these proved to be nonspecific using an indirect ELISA with human transferrin as solid-phase antigen.

The supernatants from the remaining 17 hybridoma clones (from the second fusion) were further screened by immunoblotting (Figure 2.10).

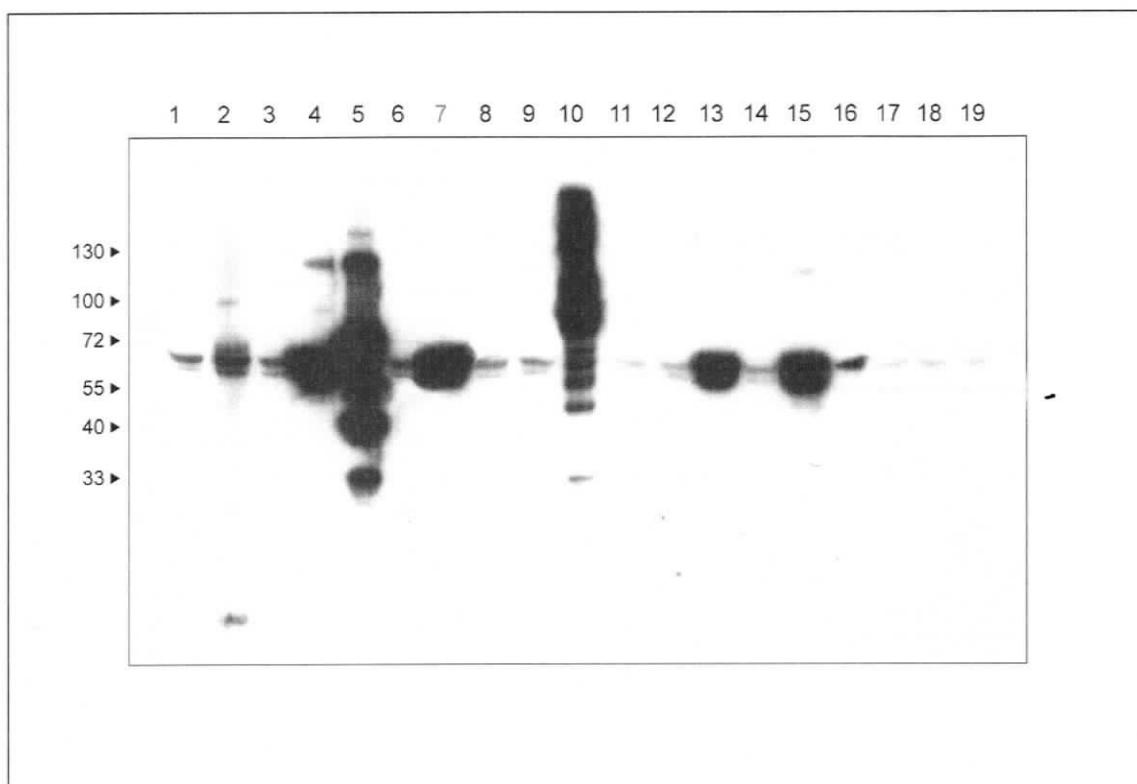


Figure 2.10 *Immunoblot analysis of monoclonal antibodies.*

*Glycoproteins from the immunogen mixture were separated using a pre-cast 12 well, 4-12% Bis-Tris gradient gel (Invitrogen), blotted onto PVDF membrane and probed with tissue culture supernatant from the hybridomas derived after the *in vivo* stimulation with the immunogen mixture. Lane numbers correspond to hybridoma supernatants used as primary antibody.*

1. 3C1	*6. 3B2	11. 3G5	16. 7C11
2. 1A10	7. 3F9	12. 3G10	17. 7D8
3. 1C9	8. 3F11	13. 5G2	18. 7E6
4. 2A10	9. 3G2	14. 6H11	19. 7E9
5. 2G7	10. anti-gp96 (+ ctrl)	15. 7B10	

**Clone from previous fusion, used as an additional positive control.*

One common banding pattern emerged from the immunoblot analysis of the hybridoma supernatants; a single band was detected at approximately 65 kDa. To identify this immunodominant antigen, the electrophoretically purified and identified glycoprotein cores from previous 2-D gels of the immunogen mixture were run on by 1-DGE and probed with several tissue culture supernatant. It was found that the common antigen was calreticulin (Figure 2.11).

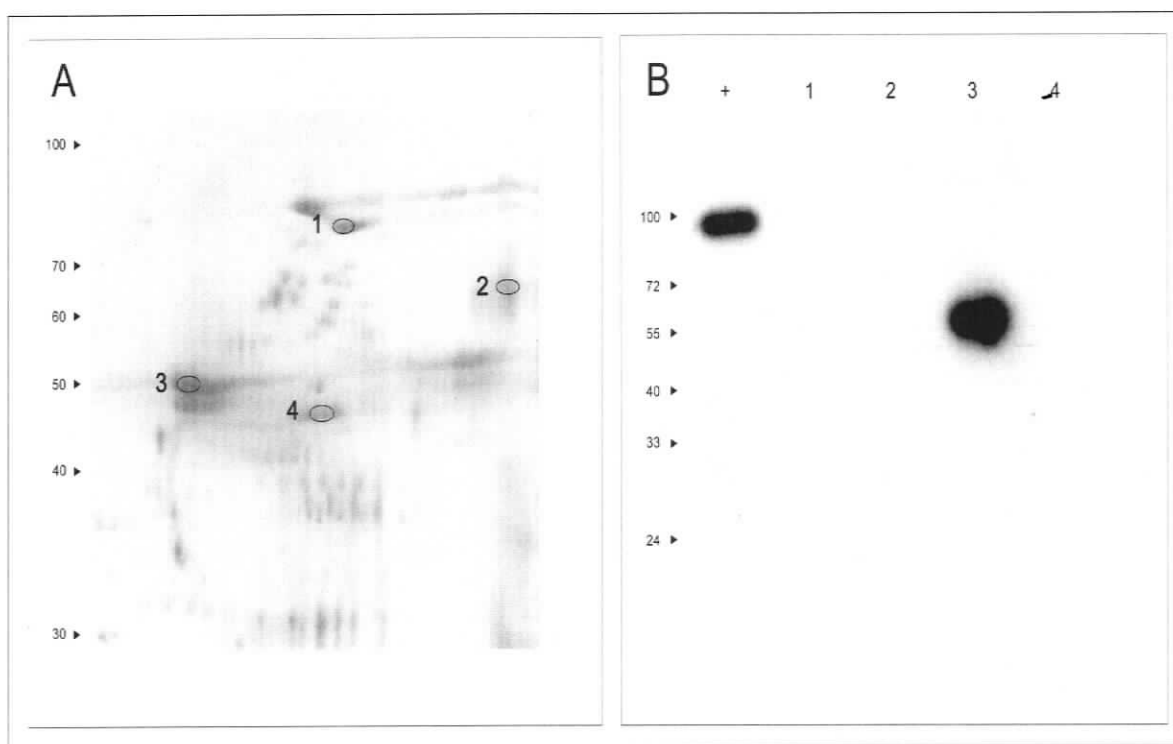


Figure 2.11 *Specificity analysis of monoclonal antibodies derived after both in vitro and in vivo immunization methods.*

Panel A: The glycoproteins in the immunogen mixture were resolved by 5-15 % gradient two-dimensional gel electrophoresis and stained with Colloidal Coomassie Brilliant Blue G-250. Selected spots were excised and prepared for identification by mass spectrometry. Ellipse 1, bovine gp96; ellipse 2, bovine transferrin; ellipse 3, bovine calreticulin and ellipse 4, ERp57. Panel B: Two-dimensional gel purified bovine chaperones were run on a 1.5 mm, 12.5 % one dimensional gel and electrophoretically transferred to PVDF membrane. The membrane was probed with tissue culture supernatant from several hybridomas developed after both the in vitro and in vivo stimulation methods to confirm their antigen specificity. Lane numbers correspond to the resolved chaperones in panel A.

Table 2.2 *Summary: monoclonal antibodies produced against bovine liver glycoproteins.*

Fusion technique	Antisera titre	Clones characterized	Positive on immunogen	Positive on human transferrin	Molecular mass of proteins recognized	Isotype
<i>In vitro</i> stimulation	1/200	672	69	30	53 kDa 80 kDa	All IgM
<i>In vivo</i> stimulation	1/200	672	38	21	65 kDa	All IgM

DISCUSSION

In an attempt to generate monoclonal antibodies against bovine gp96 and other chaperones involved in antigen presentation, a crude enrichment of glycoproteins from bovine liver tissue was performed. An isolation method loosely based on several published procedures (Meng et al. 2002; Srivastava 1997; von Bonin et al. 2003) was developed and optimized. To determine the effectiveness of this method in enriching the molecules of the antigen presentation pathway, the molecules isolated by Con A chromatography were resolved by 2-D gel electrophoresis and identified by mass spectrometry. The ER chaperones calreticulin, gp96 and protein disulfide isomerase (ERp57) were identified by peptide mass fingerprinting. It was unexpected that calreticulin was isolated by Con A chromatography as it is normally non-glycosylated. However, Matsuoka *et al* found that glycosylation of calreticulin was species as well as tissue specific, with calreticulin from bovine liver being one of four examples where this occurs (Matsuoka et al. 1994). As expected, tapasin and the MHC class I molecules were not identified, as they are transmembrane proteins not expected to be isolated by this detergent-free procedure.

Although gp96, calreticulin and ERp57 were identified in the Con A-enriched immunization mixture, an immune response to the chaperones cannot be predicted based on their presence within the immunizing sample alone. The immunogenicity of the molecule is imperative. In the production of monoclonal antibodies it is generally accepted that the greater the phylogenetic distance between antigen and host, the greater

the immune response generated. Therefore, the immunological response against highly conserved antigens will be weak, if stimulated at all (Goding 1983). Because of their integral role in antigen processing, the dedicated chaperones of the ER are highly conserved between species and therefore possibly tolerated by the immune system. The most abundant protein identified in the immunization mixture was bovine calreticulin, which shares 90 % sequence identity with its murine counterpart. Bovine and murine gp96 are 96 % similar while ERp57 from the two species are 92 % similar (alignments performed by clustalW (EMBL-EBI), Appendix II). If an immune response were to be provoked by these conserved chaperones, the epitope would likely be species specific.

The production of murine monoclonal antibodies against foreign antigens has been well studied. However, it is generally accepted that stimulating B lymphocytes to produce antibodies specific for phylogenetically conserved non-immunogenic epitopes remains difficult (Brams et al. 1987). Borrebaeck and Moller (1986) found that “*in vitro* immunized [mouse] spleen cells showed an ability to synthesize antibodies against self-antigens”. They propose that the reduced interaction with regulatory T lymphocytes in the single spleen cell suspension may be responsible for the successful immune response to conserved or self-antigens. Unfortunately, Brams et al (1987) found that while the *in vitro* antigen priming method is optimized for non-immunogenic antigens, it predominately gives rise to antibodies of the IgM isotype. This creates a problem: to create the affinity matrix for the purification of bovine chaperones, the murine mAbs are usually coupled to either protein A or protein G agarose. This procedure necessitates that the murine mAbs be of an IgG isotype. While the *in vitro* stimulation procedure of

Borrebaeck and Moller (1986) as well as the traditional *in vivo* antigen priming method were not ideal for this project, both were performed.

Cell fusions performed after the *in vitro* and *in vivo* lymphocyte stimulations resulted in more than 1000 hybridomas. Immunoblot analysis of the mAbs produced after the *in vitro* antigen stimulation method revealed three common banding patterns, a single band at approximately 50 kDa, a single band at approximately 80 kDa or a combination of both (see Figure 2.7). Prior to immunoblotting, the panel of mAbs was screened by ELISA on human transferrin (79,870 Da) and discarded if they were positive. It can therefore be assumed that the antigen at approximately 80 kDa was not transferrin or if so the epitope recognized was species-specific. The antigen seen at approximately 50 kDa was determined by mass spectrometry to be calreticulin. The 2-D gel resolved proteins: bovine gp96, transferrin, calreticulin and ERp57 were electrophoresed out of the gel plugs into a 1-D gel, the gel was blotted and probed with several hybridoma supernatants to confirm their anti-calreticulin specificity (see Figure 2.11). As predicted, the isotype of the 39 mAbs produced by the *in vitro* stimulation method and screened by immunoblotting was uniformly IgM.

Clones produced by the standard *in vivo* immunization method displayed only two banding patterns when immunoblotted against the immunogen mixture: either multiple, wide range binding or a single band at 65 kDa (see figure 2.10). Again, the isotype of all the mAbs produced by the *in vivo* stimulation procedure was IgM. Unlike the *in vitro* stimulation procedure, the *in vivo* stimulation method does not necessarily bias towards

the production of an IgM isotype, therefore, perhaps the conserved chaperone antigens themselves were responsible for the phenomenon. The cytokine environment at the site of immunization is often responsible for class switching yet the *in vivo* stimulation method is used frequently in our lab without generating predominantly IgM producing hybridomas. Coutinho, et al (1995) documented a pre-existing class of naturally occurring autoantibodies from fetal development, most of which are of IgM class. "A large proportion of these natural autoantibodies are polyreactive to phylogenetically conserved structures such as nucleic acids, heat shock proteins, carbohydrates, and phospholipids" (Boes et al. 1998). This supports the idea that the conserved chaperones themselves may be responsible for the consistent production of IgM secreting hybridomas.

In total 1344 hybridomas were characterized; 51 produced IgM antibodies specific for transferrin and 41 produced IgM antibodies specific for calreticulin. While it was assumed that hybridomas specific for several glycoproteins of the antigen processing pathway would be produced due to the complex immunogen mixture, it was interesting that none of the hybridomas characterized were specific for gp96. If the observations of Coutinho, A. et al (1995) indicate that only antibodies of IgM class will be produced to phylogenetically conserved structures, increasing the phylogenetic distance between the antigen and host may be the only way to generate IgG specific mAbs to molecules of the antigen processing pathway.

CHAPTER 3. IMMUNOAFFINITY ISOLATION OF BOVINE GP96 AND IDENTIFICATION OF BOUND PEPTIDES.

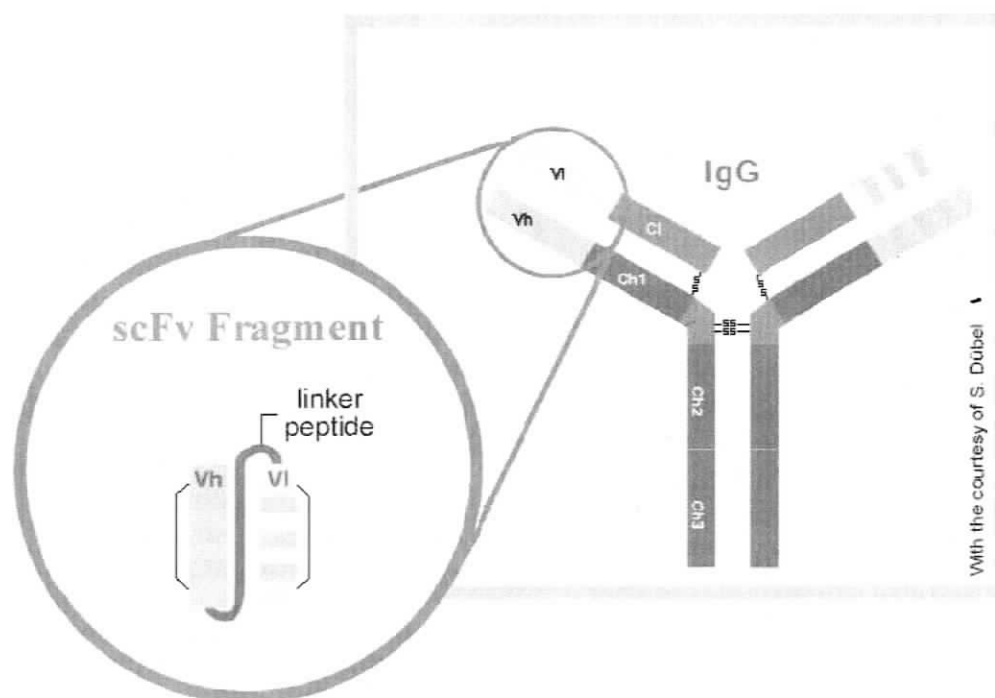
INTRODUCTION

Single chain antibodies

Immunoglobulins are molecules of the humoral immune system with the ability to specifically recognize a single antigenic site, the epitope. The prototypic antibody consists of four polypeptides, two heavy (H) chains and two light (L) chains, held in a typical Y conformation by a series of interchain disulfide bonds. The majority of the antibody structure is generated from a relatively conserved amino acid sequence, which encodes the constant portions of the antibody. This constant region encompasses all but the two amino terminal regions of the heavy and light chain dimers (the tips of the Y structure). These amino terminal variable regions impart the immunoglobulin's antigen binding specificity and are referred to as the antigen binding sites. The sequences and structure of the antigen binding sites vary greatly and this heterogeneity allows immunoglobulins to exist that are specific for an almost limitless variety of antigens.

Genetic techniques of the last decade have allowed engineering of antibodies to produce molecules retaining the variable region specificity coupled to different segments of the constant region. One such modification consists of the variable regions from one heavy chain and one light chain joined by a short peptide linker. In contrast to the native antibody, this single chain antibody fragment only contains a single antigen-binding site,

and is termed an ScFv (Single chain Fragment variable). ScFvs offer researchers the advantage of exquisite antigen specificity coupled with both a reduced size and lack of effector function associated with the antibody constant region.



Like natural, full size antibodies, the small ScFvs can be coupled to solid supports to create an affinity matrix that specifically binds a single antigen of interest. Such affinity matrices are especially useful for the isolation of antigens from complex biological mixtures under physiological conditions. In the work reported here I employed ScFv affinity chromatography to isolate gp96 from bovine liver tissue and from cell lines of several species. In this way, gp96 could be isolated under mild conditions allowing retention of its bound peptides. After the gp96-peptide complexes had been affinity

isolated, the peptides were released from the chaperone by acid treatment and differentially labeled for analysis by mass spectrometry.

Mass spectrometry

Mass spectrometry (MS) has increasingly become the method of choice for protein analysis. It requires minimal sample and couples rapid analysis with high sensitivity and specificity. In this study MS was used to analyze peptides derived from two different samples (Chapter 2); i) tryptic peptides derived from proteins resolved by two-dimensional gel electrophoresis (Chapter 3), ii) peptides isolated from affinity purified gp96 chaperone. These distinct peptide samples required the use of two specialized mass spectrometers for their analysis.

i) Trypsin digested proteins

Glycoproteins were chromatographically isolated from bovine liver tissue and separated by two-dimensional gel electrophoresis (2-DGE). The resolved glycoproteins were then individually digested with trypsin to generate a set of peptides characteristic for each protein. These peptides sets were analyzed by matrix-assisted laser desorption/ionization time-of-flight (MALDI-TOF) mass spectrometry to generate a list of their mass to charge ratios (m/z), referred to as the peptide mass fingerprint (PMF). Multiple algorithms were used to search protein databases with the PMFs to determine the identity of the parent proteins and their amino acid sequences. The search algorithms generate an *in silico* PMF for each protein in the database based on the cleavage specificity of the protease used. These theoretical PMFs are matched to the experimental PMF to generate an

identity probability score (Johnson et al. 2005). Using the PMF to identify the protein source requires that the protein (or homologue) sequence is known and accessible in the database used.

Mass spectrometers share four major components: a sample inlet, an ion source, a mass analyzer and a detector. The sample inlet for the MALDI-TOF mass spectrometer used for PMF generation is a stainless steel plate (stage) onto which multiple samples can be loaded. The samples are co-crystallized on the stage with an acidic UV-light absorbing matrix. Pulses of UV-laser light vaporize the matrix and carry the embedded peptides ions into the gas phase where their movement is controlled by electric fields. To determine the m/z of the intact peptide ions, a high positive voltage is applied to accelerate the positively charged gas-phase ions through a time of flight tube (TOF mass analyzer). The ions travel at a rate inversely proportional to their m/z ; thus the greater the ion's m/z value, the slower the ions travel. The time required to traverse the flight tube and reach the detector is measured and used to calculate the m/z of the individual ions. To increase resolution, ion mirrors or reflectrons are added to the TOF mass analyzer. A reflectron is an electric field that reverses the direction of the ions, which allows ions sharing the same m/z but different velocities to be focused and thus appear at the detector synchronously.

ii) Peptides isolated from gp96 chaperones

A complex set of peptides was isolated from murine and human gp96 chaperones and analyzed by tandem mass spectrometry (MS/MS). Differential peptide expression

analysis using iTRAQ™ (isobaric Tags for Relative and Absolute Quantitation) technology was employed to identify peptides present in one sample and not another, for example in comparing protein subsets from infected and uninfected cell lines. The two peptide subsets were each labeled with a different primary amine-specific iTRAQ™ reagent and the samples combined to enable comparison of the two samples within a single mass spectrum. Each iTRAQ™ label consists of three functional groups: a peptide reactive group, an isobaric tag and a reporter group. The peptide reactive group covalently labels free primary amines from the peptide N-terminus or lysine side chains. The reporter group is a cleavable tag of 114, 115, 116 or 117 mass units used to differentially identify the samples and the isobaric tag ensures that identical peptides originating from different samples have the same mass regardless of the additional mass of the iTRAQ™ reporter group. The reporter group is cleaved upon MS/MS fragmentation displaying distinct masses. By comparing the reporter ion intensities, the relative quantity of identical peptides from different iTRAQ™ labeled protein samples can be deduced in one experiment. Software assisted sequencing of the MS/MS peptide fragmentation data were used to search heterologous databases to deduce the identity of the parent protein.

Tandem mass spectrometers are used for the structural analysis of peptides and were utilized in the analysis of the complex mixture of gp96-chaperoned peptides. These instruments have more than one mass analyzer, each performing separately to generate data from sequential stages of the analysis. The first mass analyzer separates the mixture of gas phase ions based on their m/z ratio to generate a spectrum (survey scan) of all the

ions present in the sample. In the second mass analyzer, a precursor ion of interest is selected from the survey scan and electromagnetically steered into a collision cell. By introducing enough energy into the targeted peptide, it can be induced to fragment at established vulnerable regions of the peptide backbone. The fragmentation pattern reflects a stepwise reduction in the amino acids that structure the peptide. Masses corresponding to the intact peptide and the fragments reflecting the sequential loss of individual amino acids are used to determine the primary sequence of the parent peptide and finally the identification of the parent protein (Figure 3.6 and Table 3.1).

A MALDI TOF/TOF (Applied Biosystems/MDS SCIEX model 4800) tandem mass spectrometer was used in the analysis of gp96 associated peptides. This analyzer was optimal due to its high-energy collision cell that optimizes the fragmentation of the naturally occurring peptides isolated from gp96. Classically, mass spectrometric analysis of proteins involves controlled sample degradation by trypsin cleavage, which results in a nested set of peptides with a fixed C-terminal positive charge. The presence and location of this charge aids in complete fragmentation and therefore yields informative MS/MS data. The naturally occurring MHC class I destined peptides isolated from gp96 do not necessarily possess a fixed C-terminal positive charge, therefore their optimal MS/MS fragmentation requires the higher energy collision cell offered in the MALDI TOF/TOF mass spectrometer.

The MALDI TOF/TOF uses a single TOF mass analyzer therefore sequential mass analysis occurs temporally rather than spatially. Chromatographic separation of complex

peptide samples is performed off line in this arrangement and the fractionated sample is co-crystallized with matrix and ionized by laser pulsing as in the MALDI TOF mass spectrometer described above. The plume of peptide and matrix ions extracted by the laser pulse is accelerated into the first TOF mass analyzer after a pre-determined time delay. This time delay increases resolution by allowing all ions of the same m/z ratio to reach the detector synchronously regardless of their initial extraction velocity and location within the sample. A peptide of interest is selected from the survey scan and steered into the high-energy collision cell where it is collided with an inert gas (usually air) causing fragmentation. These peptide fragments are re-accelerated into the TOF tube (second mass analysis) where they are reflectron-focused to increase resolution before reaching the detector. The product ion spectrum of the peptide fragments generated allows software assisted sequencing of the targeted peptide. By combining the peptide mass obtained from the precursor scan and the sequence data obtained from the fragmentation spectrum the origin of the peptide can be determined. The MS/MS fragment mass lists generated are submitted to both BLAST and MASCOT databases for determination of protein identity.

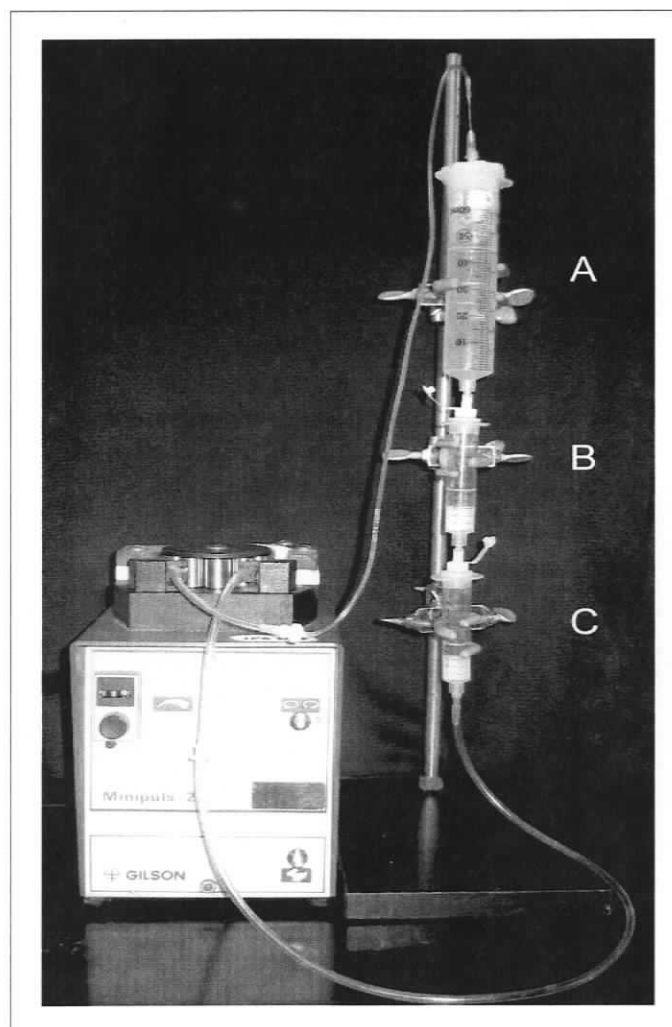
My strategy is to immunoaffinity isolate gp96 associated peptides from a *T. parva* infected bovine T lymphocyte sample and an uninfected matched bovine T cell line. The two sets of peptides will then be differentially labeled to allow their comparative analysis by MALDI TOF/TOF MS/MS.

MATERIALS AND METHODS

3.1 Affinity purification of gp96 chaperone from murine EL4, human Jurkat and *Theileria parva*-infected and uninfected bovine cell lines.

Murine EL4 thymoma and human Jurkat cell lines were cultured in suspension in 4 L spin flasks to an average density of 5×10^5 cells per mL. Uninfected and *Theileria parva*-infected bovine cell lines were cultured and lysates prepared by our collaborator Dr. Ivan Morrison and his staff at the University of Edinburgh, Scotland, UK. All cell lines were lysed on ice in hypotonic lysis buffer (30 mM NaHCO₃ supplemented with 1 μ M Pepstatin A (final concentration) and protease inhibitor cocktail (Protease Inhibitor Cocktail Set V, EDTA-Free, Calbiochem, La Jolla, CA). To ensure complete cell lysis, samples were dounce homogenized on ice in 5 mL fractions and the lysates cleared by centrifugation at 2,100 x g for 30 min at 4 °C (Heraeus Sepatech tabletop centrifuge, Heraeus, Osterode, Germany). The supernatants were transferred to polyallomer centrifuge tubes (Beckman, Palo Alto, CA) and ultracentrifuged at 100,000 x g at 4 °C for 90 min using a Beckman L8-70 Ultracentrifuge (Beckman, Palo Alto, CA) to obtain the gp96-containing soluble fraction. Soluble fractions were allowed to recirculate over a manually poured anti-human serum albumin ScFv affinity column (to pre-clear the sample of non-specifically adhering proteins) and an anti-gp96 ScFv affinity column arranged in series using Luer-lock mini columns (Mo Bi Tec Molecular Biotechnology, Goettingen, Germany). The samples were recirculated at 4 °C overnight at a flowrate of 1 mL/min using a Gilson peristaltic pump (Gilson Minipuls 2; Mandel Scientific Company Inc, Guelph, ON). The single chain antibody (ScFv) affinity resins were

prepared in collaboration with Christian Kleist of the Hansjorg Schild lab at the Institute for Cell Biology, Department of Immunology, University of Tübingen, Heidelberg, Germany.



Configuration of the peristaltic pump, sample inlet chamber (A), anti-HSA affinity column (B) and anti-gp96 ScFv affinity column (C)

The columns were washed with 10 mL PBS before block elution using 6 mL volumes of: 0.25 M NaCl in PBS, 0.5 M NaCl in PBS, PBS (no additional salt) and 1.3 M NaCl in PBS. The columns were eluted separately into 1.5 mL Maxymum Recovery

microcentrifuge tubes (Axygen Scientific, Union City, CA) on ice using 10 mL luer-lock syringes. After the columns were eluted they were cleaned using a solution of 2.0 M NaCl in PBS and stored in PBS containing 0.02 % sodium azide for reuse with the same cell line. Ten μ L of each fraction (6 fractions per elution buffer) were run on a 1-D SDS-PAGE gel and immunoblotted using an anti-gp96 monoclonal antibody (Stressgen Biotechnologies, Victoria, Canada) to determine the gp96 containing fractions. The eluates obtained using 0.5 NaCl in PBS, the PBS wash and the 1.3 M NaCl in PBS elution contained gp96 and were therefore pooled for acidification and further analysis of released peptides.

3.2 Immunoblotting.

Immunoblotting using BioTrace™ polyvinylidene difluoride (PVDF) membrane (Pall Corporation, Ann Arbor, MI) was performed essentially as previously described (Beecroft et al. 1993) with the exception of increased transfer time to 45 min and the substitution of a more sensitive substrate (SuperSignal West Dura chemiluminescence substrate; Pierce Chemical Company, Rockford, IL). A 1:1,000 dilution of the positive control antibody (rat anti-Grp94; SPA-850, Stressgen Biotechnologies, Victoria, BC) and 1:2 dilutions of hybridoma tissue culture supernatants were used as primary antibodies and a 1:50,000 dilution of secondary antibody (goat anti-rat IgG-horseradish peroxidase conjugate; Cedarlane Laboratories Ltd., Hornby, ON) was employed. Kodak Biomax MR film (Eastman Kodak Company, Rochester, NY) was used to detect chemiluminescence. After development of the autoluminograms, proteins were stained on the PVDF membrane with GelCode® Blue (Pierce Chemical, Rockford, IL). The

exposed film was superimposed on the stained PVDF membrane to reveal the precise location of the immunoreactive protein bands in relationship to the entire protein profile.

3.3 Peptide elution and reversed-phase C18 column chromatography.

The pooled affinity column fractions containing gp96 were acidified using 6M guanidine-HCl, 0.2 % TFA to strip bound peptides from the chaperone. The acidified samples were incubated at 37 °C for 30 min and cooled to room temperature before further processing (Liu et al. 2004). Intact gp96 protein was removed from the peptide samples using disposable Altech High Capacity SPE C18 columns (Altech Associates, Guelph, ON) according to the instructions of the manufacturer. The solid phase extraction of the peptides was performed at a flow rate of 1 mL/min using a PrepSep™ vacuum manifold (Fisher Scientific, Ottawa, Canada). The acidified samples were allowed to flow over the column three times to optimize binding before peptide elution with 50 % ACN, 0.1 % TFA. The eluates were brought to dryness using a Speed Vac Concentrator (Savant, Hicksville, NY).

3.4 iTRAQ™ peptide derivitization.

Differential labeling of the isolated gp96-associated peptides was performed with the primary amine-specific iTRAQ™ reagent (Applied Biosystems, Foster City, CA) as described by the manufacturer. Changes to the protocol included using 30 µL of dissolution buffer to correct for initial sample volume and omitting the addition of denaturant (2 % SDS) to allow compatibility with reversed phase chromatography. The labeling reaction was allowed to proceed at room temperature for 1.5 hours.

3.5 Peptide fractionation by reversed phase chromatography.

An integrated system consisting of a Famos autosampler, Switchos II switching pump and Probot automated sample spotting robot (LC Packings, Amsterdam, Netherlands) was used for the further separation and characterization of the peptides isolated from gp96. Chromatographic separation of the sample was achieved on a 75 μm x 15 mm C18 PepMap Nano LC column (5 μm , 100 A) protected with a 300 μm x 5 mm C18 PepMap guard column (5 μm , 100 A) (LC Packings, Amsterdam, Netherlands). Samples were diluted in 2 % acetonitrile, 0.05 % TFA and transferred to autosampler vials (LC Packings, Amsterdam, Netherlands) and 27 μL of the sample were injected and allowed to equilibrate on the guard column for 10 min. To elute the hydrophobically bound peptides, a 33 min linear gradient from 5 % to 60 % buffer B (0.05 % TFA in 98 % acetonitrile) with a flow rate of 200 nL/min was used. To clean and recondition the column, the % B was increased from 60 % to 80 % in 2 min, held at this concentration for a further 3 min and decreasing to 5 % in 2 min where it remained for 10 min before the next sample was injected. Peptides eluting from the nanobore-reversed phase column were spotted onto Opti-TOF 96 well MALDI TOF/TOF sample plates (Applied Biosystems/MDS SCIEX) in 1 min (200 nL) fractions.

3.6 Tandem mass spectrometry.

The fractionated, differentially labeled peptides were analyzed using a model 4800 MALDI TOF/TOF Analyzer (Applied Biosystems/MDS SCIEX) fitted with a 200 Hz Nd:YAG laser operating at 355 nm. The mass spectra were acquired in delayed extraction, positive reflectron mode. External calibration was performed on the precursor

ion using a standard mix of six peptides: des-Arg1-Bradykinin (m/z 904.468), Angiotension1 (m/z 1296.685), Glu1-Fibrinopeptide (m/z 1570.677), ACTH 1-17 (m/z 2093.087), ACTH 18-39 (m/z 2465.199) and ACTH III 7-38 (m/z 3657.929). MS/MS spectra were acquired from 1400 consecutive laser shots.

3.7 Database searching.

MS/MS database searching was performed using MASCOT version 1.4.1 and BLAST (<http://www.ebi.ac.uk/blast/>) algorithms. MASCOT was used with the following parameters: 100 ppm peptide tolerance, 0.1 Da fragment tolerance and no missed cleavages. Fixed modifications consisted of (N-term) iTRAQ, Lysine (K) iTRAQ and MMTS (C) and variable modifications of Tyrosine (Y) iTRAQ and Oxidation (M). The MSDS database chosen was restricted to mammals. BLAST was used with the following parameters: 0.1 Da mass tolerance, unknown enzyme, no missed cleavages with fixed modifications and variable modifications identical to Mascot. The peptide sequences obtained from BLAST were downloaded to the protein database NCBIInr (restricted to mammals) to assign the probable parent protein.

3.8 Micro-dot blotting.

Micro-dot blots were performed using nitrocellulose discs (BioTrace® NT Pure nitrocellulose blotting membrane, Pall Corporation, Ann Arbor, MI) prepared using a standard three-hole punch. The discs were labeled using a sharp pencil before 5 μ L of the gp96-containing protein aliquots were spotted; one sample per nitrocellulose disc. The antigen loaded discs were dried at room temperature and inserted into standard 96-

well plates, oriented perpendicular to the working surface. Immunodevelopment was performed in the 96-well format to reduce reagent volumes. The immunoreactions were performed as described in the immunoblotting method outlined in Chapter 2. Stock anti-gp96 ScFv Clone BioC (2.0 mg/mL) was diluted in 5 % skim milk in PBS containing 0.1 % TWEEN-20 (blocking buffer) and goat anti-c-myc secondary antibody (Stressgen Biotechnologies, Victoria, BC) was diluted to 1:75,000 in 5 % blocking buffer. Optimal removal of unbound antibodies was obtained by washing the nitrocellulose discs together in a large dish.

RESULTS

An anti-gp96 ScFv affinity resin, obtained from our collaborator in Heidelberg Germany, Christian Kleist, was used to affinity purify gp96 under physiological conditions from glycoproteins enriched from several cell lines. Gp96 containing eluate fractions were identified by immunoblotting (Figure 3.1).

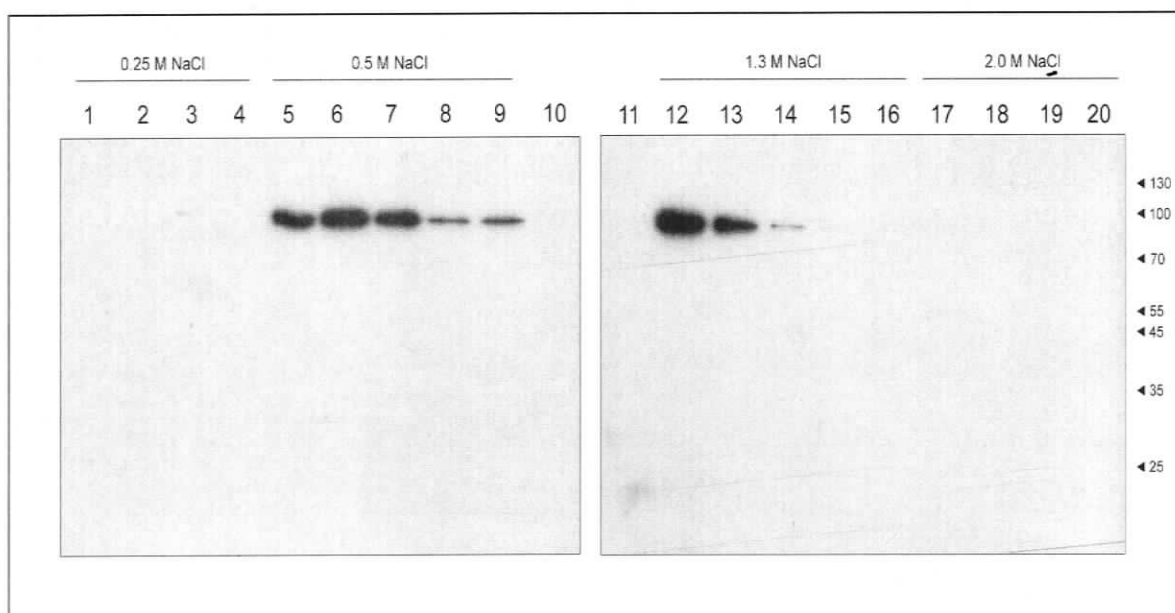


Figure 3.1 *Immunoblot analysis of gp96 ScFv affinity purified from Mus musculus EL4 cell line.*

Proteins eluted from the anti-gp96 ScFv affinity column were separated using a 10 % gel, blotted onto PVDF membrane and probed with anti-gp96 monoclonal antibody (Stressgen). Lanes 1-4 represent fractions of 0.25 M NaCl eluate; lanes 5-9, 0.5 M NaCl eluted fractions; lanes 12-16, 1.3 M NaCl eluted fractions; and lanes 17-20, 2.0 M NaCl elution fractions.

The complexity of the gp96 positive fractions was assessed by staining the PVDF membrane with GelCode Blue, which revealed that the method resulted in the acquisition of visually pure chaperone (data not shown). These fractions were pooled, the peptides acid-eluted from the gp96 chaperone and the gp96 protein removed from the peptide sample by reversed phase chromatography on a gravity flow C18 column. Differential labeling of the natural peptide sample preceded further fractionation to reduce complexity and increase peptide identification probability by mass spectrometry analysis.

Prior to mass spectrometry analysis of the natural gp96 peptides, the matrix recipe and sample deposition technique were optimized. The natural peptides associated with gp96 are reasoned to be comparable or greater in length than the 8-13 aa MHC class I-associated peptides. Assuming an average amino acid mass of 110 Da the peptides should concentrate in the 880 to 1430 m/z (singly charged) region. Therefore, spectra showing reduced low mass noise and increased peptide intensity in the low to mid mass region are optimal for the natural peptide samples isolated from gp96. Figure 3.2 summarizes spectra obtained by ionizing tryptic bovine serum albumin (BSA) peptides using three concentrations of α -cyano-4-hydroxycinnamic acid (CHCA) in a matrix base consisting of 50 % ACN, 0.1 % TFA. The figure illustrates a reduction from 10 mg/mL to 3 mg/mL CHCA resulting in an overall increased signal to noise ratio coupled with reduced interference by low mass range matrix peptides. The data also highlight an increase in peptide intensity in the 1000 to 2700 (m/z) (low to mid) mass region with a 140 % increase in detectable peptides when acquiring data using 3 mg/mL CHCA compared 10 mg/mL CHCA (panel C vs panel A).

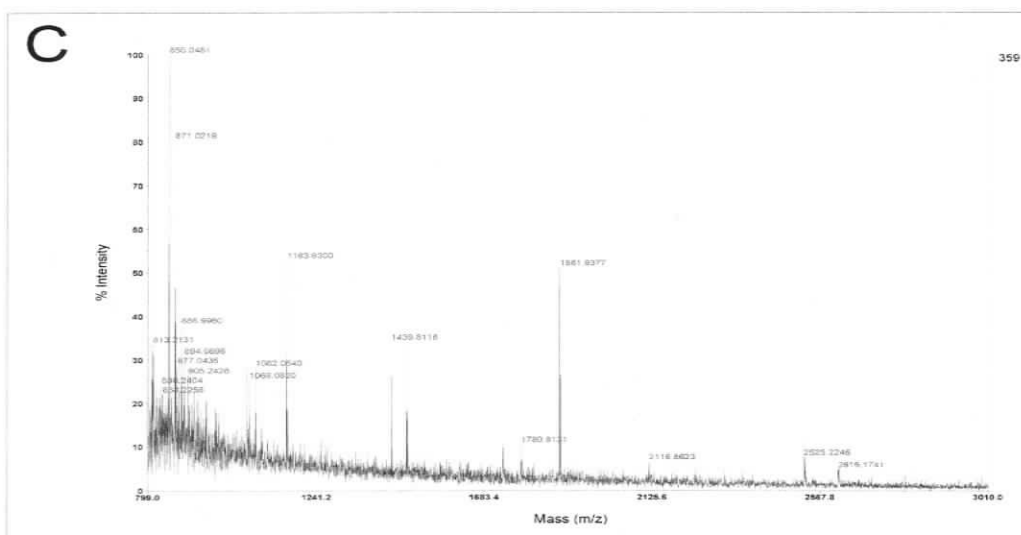
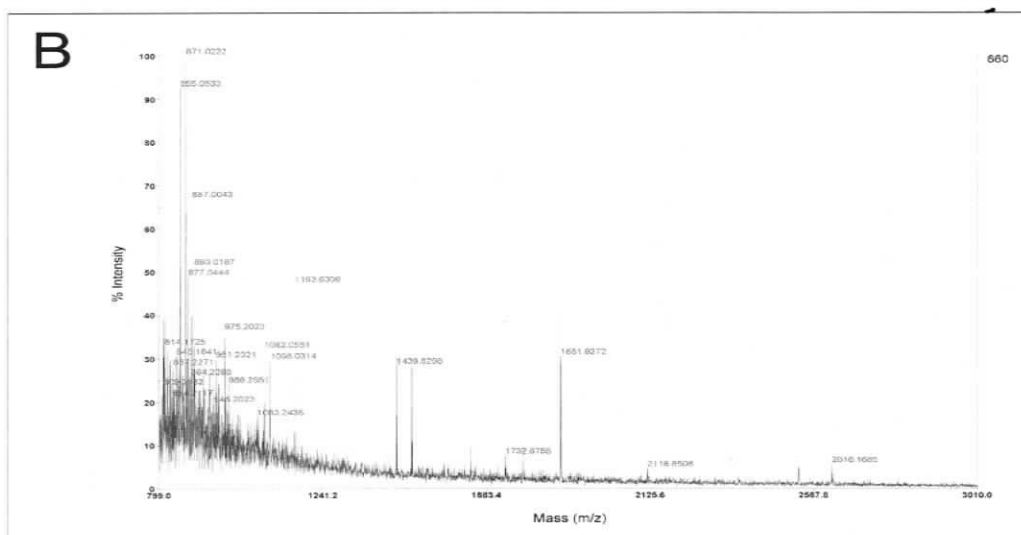
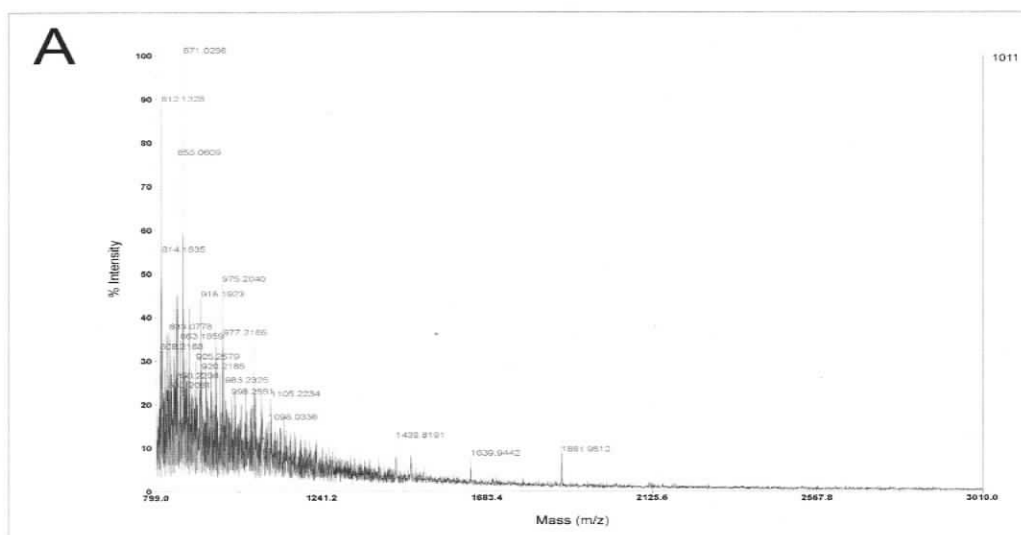


Figure 3.2 Optimization of MALDI TOF/TOF CHCA matrix concentration.

MALDI TOF/TOF mass spectra (positive reflectron mode) of BSA tryptic peptides recorded using three concentrations of CHCA in a sample matrix containing 50% ACN, 0.1 % TFA. One μL of matrix was allowed to dry before the 100 fmol digested BSA sample was applied. Panel A, 10 mg/mL CHCA; panel B, 5 mg/mL CHCA; panel C, 3 mg/mL CHCA.

To further improve the signal to noise ratio by reducing matrix adducts (Zhu and Papayannopoulos 2003), 8 mM ammonium citrate was added to matrices comprised of the three concentrations of CHCA assessed in Figure 3.1. The addition of 8 mM ammonium citrate made a substantial difference to the low mass range baseline and increased the overall peptide intensities. Optimal spectra were obtained using a combination of 3 mg/mL CHCA with 8 mM ammonium citrate (see Figure 3.3, panel C). Further optimization of the matrix recipe was attempted by increasing the 3 mg/mL CHCA matrix organic concentration from 50 % to 90% in 10 % increments. The resulting data did not reveal additional tryptic peptides nor did they show a further decrease in the baseline (data not shown).

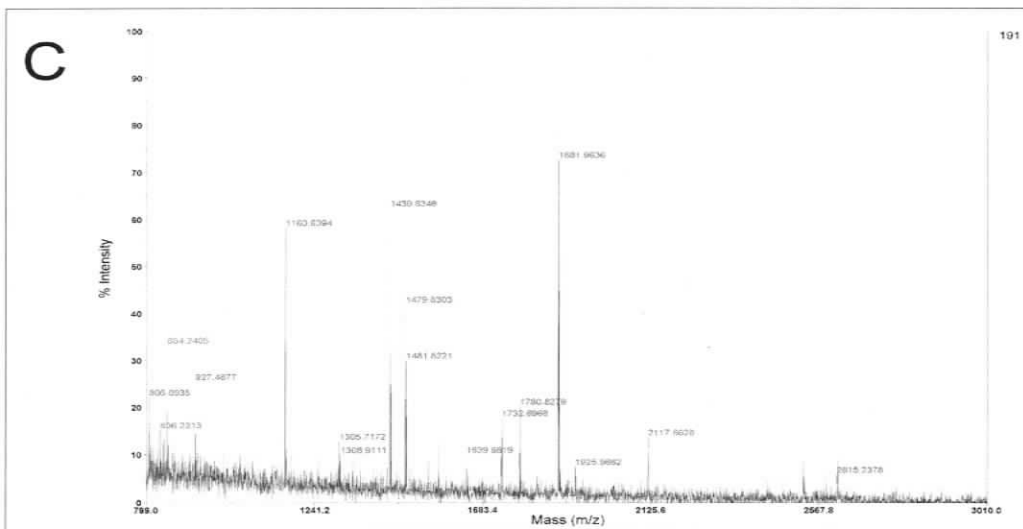
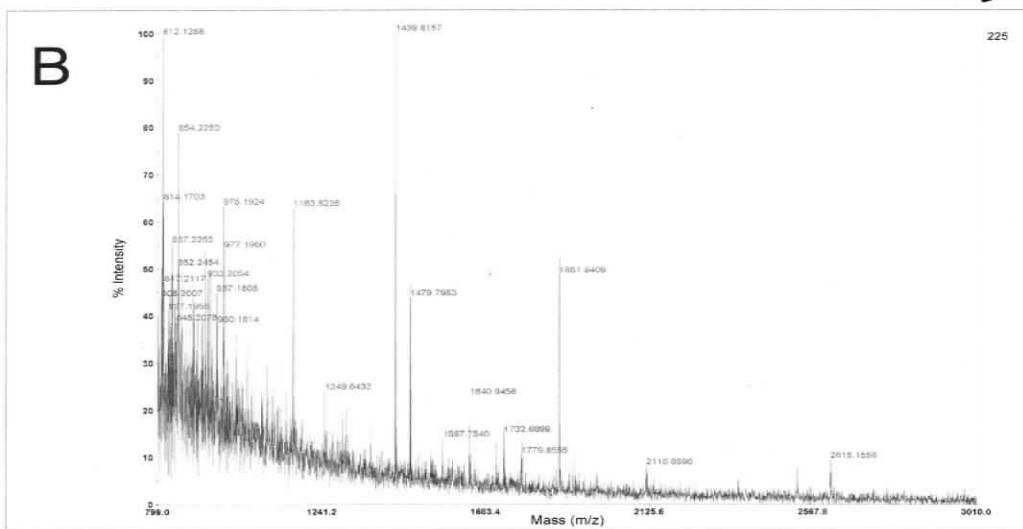
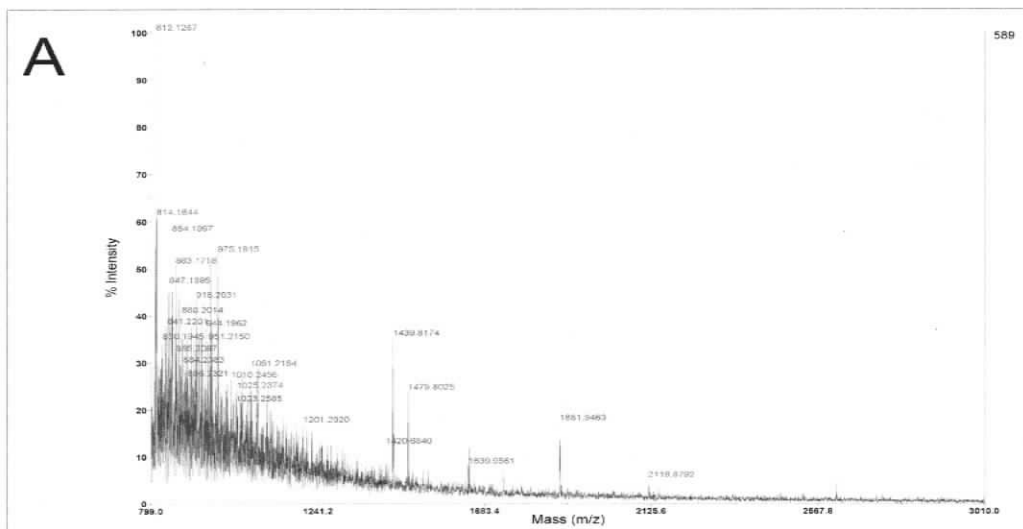


Figure 3.3 *Effects of ammonium citrate addition to MALDI TOF/TOF CHCA matrix.*

MALDI TOF/TOF mass spectra (positive reflectron mode) of BSA tryptic peptides recorded using different concentrations of CHCA in a sample matrix containing 8 mM ammonium citrate, 50 % ACN, 0.1% TFA. One μL of matrix was allowed to dry before the 100 fmol digested BSA sample was applied. Panel A, 10 mg/mL CHCA; Panel B, 5 mg/mL CHCA; Panel C, 3 mg/mL CHCA.

Samples for MALDI TOF/TOF analysis can be combined with CHCA matrix in a variety of methods. The three sample deposition techniques investigated in my research were chosen in part because of their compatibility with the Probot automated sample spotting robot utilized in the off-line C18 fractionation prior to MS/MS analysis. Each addition of sample or matrix was allowed to dry before further layers were added. Figure 3.4, panel A shows the BSA tryptic peptide spectrum obtained with an open-faced sample deposition technique (matrix then sample). When compared to the open-faced method, sample deposition using the I.D.I. (sample then matrix, panel B) or sandwich (matrix-sample-matrix, panel C) techniques resulted in an extreme increase in detectable BSA peptides. A comparable number and intensity of peptides was acquired utilizing either the I.D.I or sandwich methods. The I.D.I. technique was adopted for further sample analysis, as it requires less preparation time than the sandwich method.

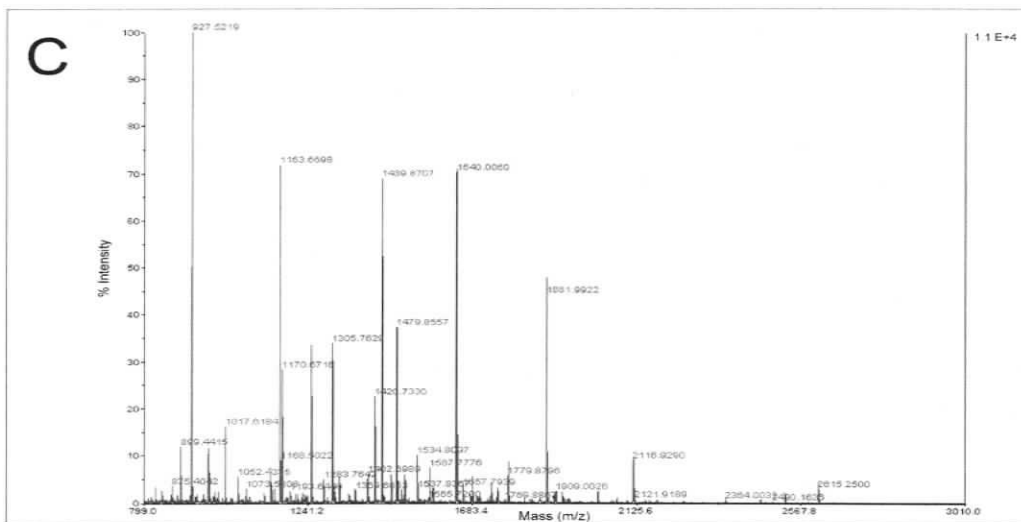
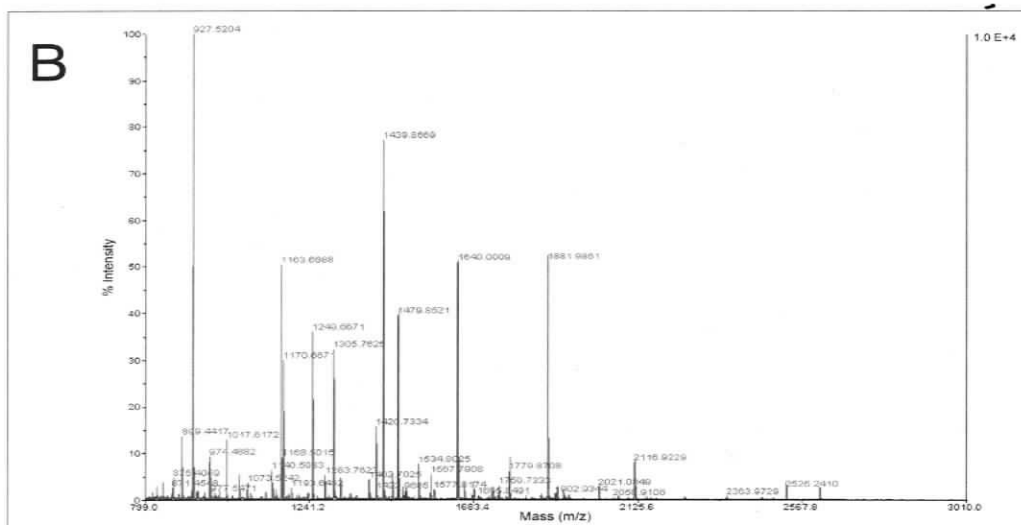
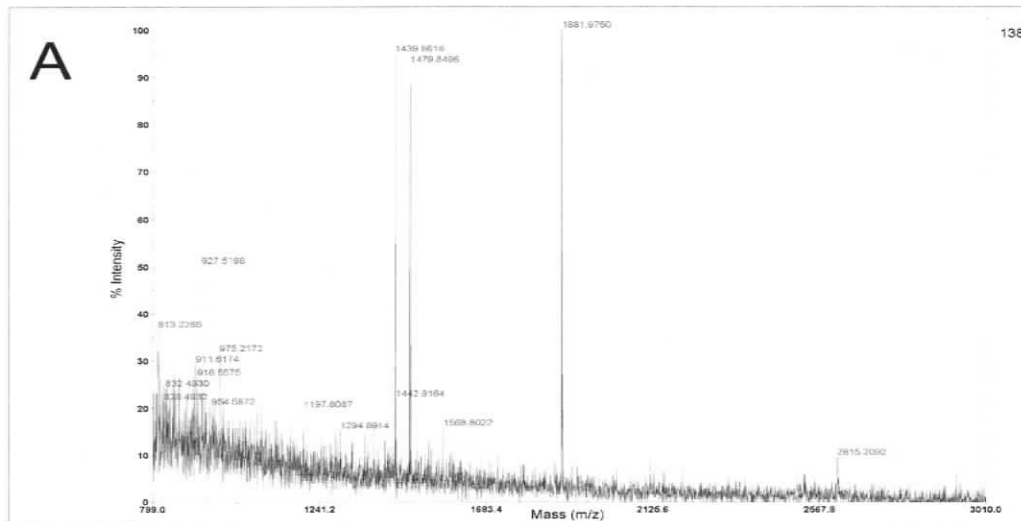


Figure 3.4 Optimization of MALDI TOF/TOF sample and CHCA matrix deposition technique.

MALDI TOF/TOF mass spectra (positive reflectron mode) of BSA tryptic peptides obtained using three sample deposition techniques. The matrix (3 mg/mL CHCA, 8 mM ammonium citrate, 50 % ACN, 0.1% TFA) and sample were allowed to dry before the addition of further layers. Panel A: 1 μ L matrix followed by 1 μ L digested BSA sample (open-faced). Panel B: 1 μ L matrix, 1 μ L digested BSA sample and 1 μ L matrix (sandwich). Panel C: 1 μ L digested BSA sample followed by 1 μ L matrix (I.D.I).

Labeling of BSA tryptic peptides was accomplished using the primary amine specific iTRAQ™ reagent. The spectra were obtained using 3 mg/mL CHCA, 8 mM ammonium citrate, 50 % ACN, 0.1 % TFA matrix co-crystallized with the sample using the I.D.I. technique. To most accurately deduce the efficiency of the iTRAQ™ labeling experiment, the volume and chemical environment of the BSA tryptic peptide sample approximated the conditions used with the *T. parva* infected and uninfected bovine lymphocyte samples (Figure 3.5, panel A). Successful iTRAQ™ labeling was confirmed by the presence and intensity of the 116-reporter ion seen in panels B and C. To optimize the product ion spectra, fragmentation of the 1857.9169 parent peptide ion (panel A, arrow) was evaluated with and without collision induced dissociation (CID) gas (panels C and B respectively). The intensity of the peaks present in the low mass range, including the iTRAQ™ reporter ion, were greater with CID gas on during fragmentation (panel C) as compared to fragmentation with the CID gas off (panel B). The increase in low mass range peaks did not alter the overall fragmentation landscape or intensity of the mid to high mass range fragment ions.

Figure 3.5 Optimization of MALDI TOF/TOF fragmentation of iTRAQ™ labeled BSA peptides.

MALDI TOF/TOF spectra (positive reflectron mode) of BSA tryptic peptides labeled with iTRAQ™ 116. Panel A: MS spectrum in the m/z range 799 to 3010 indicating the 1857.9169 peptide chosen for fragmentation (see arrow). Panel B: MS/MS spectrum showing the iTRAQ™ 116 signature ion (asterisk) and fragmentation of the 1857.9169 BSA peptide with CID gas off. Panel C: MS/MS spectrum showing the iTRAQ™ 116 signature ion (asterisk) and fragmentation of the 1857.9169 BSA peptide with CID gas on.

In an attempt to model a *T. parva* infected bovine lymphocyte sample, gp96 peptides isolated from 1×10^8 *Homo sapiens* Jurkat cells were labeled using iTRAQ™ reagent and added to 1×10^9 labeled *Mus musculus* EL4 thymoma cells. The differentially labeled peptide mixture was fractionated off-line using nanoscale C18 reverse phase chromatography before MALDI TOF/TOF analysis. ITRAQ™ labeled peptide ions were identified in 7 of the 36 collected fractions. Figure 3.6 panel A shows the mass spectrum from one chromatographic fraction and indicates the peptide ion chosen for fragmentation in the presence of CID gas (arrow). Panel B reports the corresponding product ion spectrum for the fractionated m/z 1784.8325 peptide ion outlining the iTRAQ™ label (asterisks) and *de novo* sequence. The reported sequence was obtained with agreement using both Mascot and BLAST algorithms and was identified as *Mus musculus* γ -box binding protein.

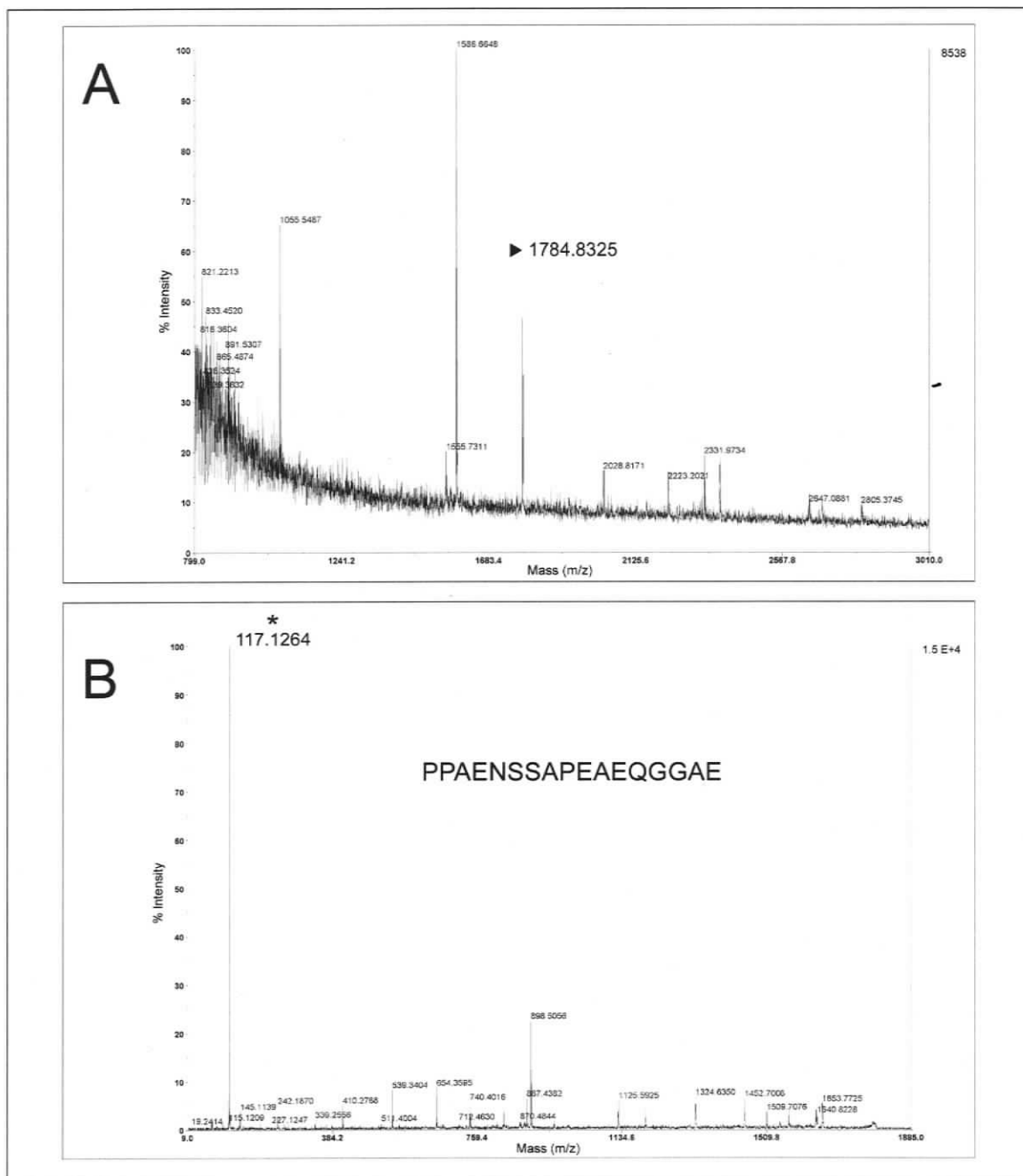


Figure 3.6 *Differential labeling and peptide sequence identification using a MALDI TOF/TOF analyzer.*

MALDI TOF/TOF spectrum of iTRAQ™ 117 labeled Mus musculus gp96 peptides isolated from 1×10^9 EL4 cells and spiked with iTRAQ™ 115 labeled Homo sapiens gp96 peptides isolated from 1×10^8 Jurkat cells. The differentially labeled peptide pools were combined and fractionated off-line by nano-flow C18. 200 nL fractions were spotted onto a MALDI sample plate and overlaid with 1 μ L CHCA matrix (3 mg/mL CHCA, 8 mM ammonium citrate, 50 % ACN, 0.1 % TFA). Panel A, MS spectrum (positive reflectron mode) of one C18 fraction indicating the 1784.8325 peptide chosen for fragmentation (arrow). Panel B, MS/MS spectrum (CID on) highlighting the 117 iTRAQ™ signature ion (asterisk) and de novo sequence. Reported sequence of the parent peptide was obtained from both MASCOT and BLAST.

Table 3.1 is a summary of the identity and sequence of iTRAQ™ labeled peptides identified from the model sample using both BLAST and Mascot search algorithms. Additional iTRAQ™ labeled peptides were identified but software assisted or manually derived sequence could not be assigned.

Figure 3.1 Summary of identified iTRAQ™ labeled peptides, their *de novo* sequence and their identity obtained using BLAST and MASCOT algorithms.

PARENT PEPTIDE (m/z)	iTRAQ™ LABEL	BLAST ID	MASCOT ID
1051.7	115	Human mucin LPVKLGH	-
1248.6	117	-	40S ribosomal protein (Mus) Acc: RS3A_MOUSE GYEPPVQESV
1586.6	117	GTPase regulator (Mus)	Alpha tubulin (Mus) Acc: AAH83344 SVEGEGEEEGEEY
1784.8	117	Y box binding protein (mus) Acc: X57621.1 PPAENSSAPEAEQGGAE	Y box binding protein (mus) Acc: CAA40847 PPAENSSAPEAEQGGAE
1847.9	115	Human protein AQLCDFWVKPY	-
1899.8	117	mKIAA2026 protein (Mus) PGDRVEEEPEELVE	Erp99 (Mus) Acc: A29317 PEAQVEEPEEPEPED
2028.8	117	Retrotransposon (Mus) AGCPLKDMGEEAEQNS	Beta tubulin (Mus) Acc: AAA40510 ATAEEEEDFGEEAEAAA
2029	117	Unknown mouse protein	Beta-tubulin (Mus) Acc: AAA40510 ATAEEEEDFGEEAEAAA
2331.9	117	IgG kappa variable region (Mus) DGPRVEDDCVTYFCLYG	Erp99 (Mus) Acc: A29317 PEAQVEEPEEPEPEDTSED
2378.0	117	-	Alpha tubulin (Mus) Acc: AAH83344 YEEVGVDSVEGEGEEEGEEY
2636.1	117	Mouse unknown protein NSVVMGKDEMVDHAFQYMS	-

Differentially labeling peptides from a complex sample and their analysis by tandem mass spectrometry was able to provide identity and sequence data in the model system established during method development. The procedure was then applied to 5×10^8 *T. parva* infected and uninfected bovine lymphocytes. The samples were obtained as cell lysates, necessitating the ScFv affinity chromatographic isolation of gp96. To confirm the cross-reactivity of the anti-gp96 ScFv with bovine gp96, known only to react with mouse and human gp96, bovine liver glycoproteins were probed with a dilution series of the anti-gp96 antibody fragment. The results in Figure 3.7 show that the anti-gp96 ScFv does detect bovine liver gp96 and retains activity to a dilution of 1:16 000 (Figure 3.7, row A).

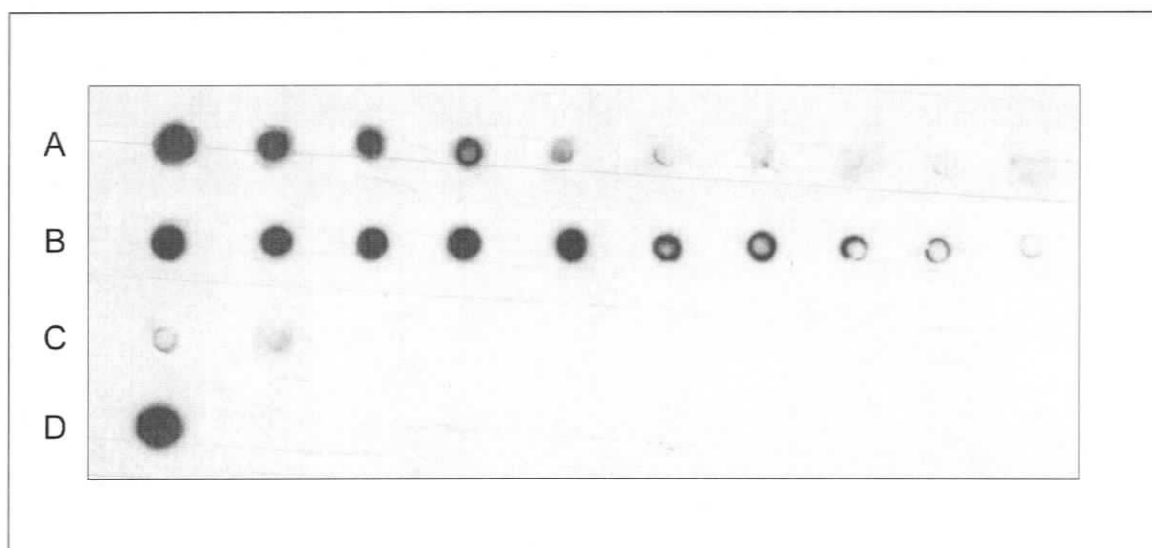


Figure 3.7 *Micro-dot blot analysis of anti-gp96 ScFv species specificity.*

Mico-dot blots were performed using Con A enriched bovine liver glycoproteins. The high carbohydrate Con A elution buffer was exchanged for PBS using gel permeation chromatography and the volume reduced by lyophilization. Five μL of the bovine liver glycoprotein solution were spotted down as antigen, and probed with two-fold dilution of antibody starting at 1:1000. Row A; anti-gp96 ScFv, row B; rat anti-gp96 (Stressgen Biotechnologies), row C; isotype-matched negative controls (showing background binding) and row D; positive control.

Gp96 from both *T. parva* infected and uninfected bovine lymphocyte cell lines was successfully isolated as determined by immunoblotting (data not shown). The gp96 samples were processed (peptides were eluted, differentially labeled and fractionated) before assessment by tandem MS/MS. Unfortunately, analysis of the fractionated sample showed that peptides were not present at detectable levels. Since this material was from our only sample, the use of *T. parva* cell lines was not continued.

DISCUSSION

A procedure to isolate, differentially label and analyze natural peptides chaperoned by gp96 was developed. The first stage validated in this multi-step method was the purification of the gp96 chaperone. Using an anti-gp96 ScFv affinity resin provided by our collaborator Christian Kleist, in Heidelberg, Germany, an affinity chromatography approach using physiological conditions was optimized for the single step isolation of gp96 molecules. The elution of *Mus musculus* gp96 was followed by immunoblotting (Figure 3.1), which confirmed that the chaperone was released from the affinity matrix within defined salt concentrations. Prior to mass spectrometric analysis of the natural peptides associated with gp96, they were acid eluted from the chaperone and the intact gp96 protein removed by C18 reversed phase column chromatography.

To facilitate comparison between gp96-associated peptides from *T. parva* infected and uninfected bovine lymphocytes, effective labeling of the peptides using the iTRAQ™ primary amine specific reagent was necessary. In addition to the ability to differentially label and compare two samples, the isobaric labeling was able to provide further information. The iTRAQ™ reagent specifically binds free amino groups of peptides therefore confirming the proteinaceous nature of a natural peptide sample that could be mistaken for matrix molecules due to their potentially small m/z values. In my model experiment, where peptide samples originating from different species were differentially labeled and combined, knowledge of the iTRAQ™ label associated with each species increased confidence in the algorithm-assigned species designation of the labeled

peptides. Peptides taken from a naturally processed gp96 source are not necessarily processed with a C-terminal positive charge as obtained with tryptic cleavage. There are theories that claim the addition of a fixed charge to either end of a peptide aid in complete fragmentation (Purcell and Gorman 2004). Since iTRAQ™ labeling imparts a charge to peptides this additional charge should therefore optimize the acquisition of sequence rich fragmentation data.

Analysis of the natural peptides eluted from affinity isolated gp96 chaperone was performed by MALDI TOF/TOF mass spectrometry. Due to the nature of the matrix used, there is an inherent tendency to mask less abundant low to mid m/z peptide ions by matrix-specific background noise. The pool of gp96-chaperoned peptides to be analyzed by tandem MS/MS was anticipated to contain peptides of similar length (from 8-20 aa), which would therefore appear in the low to mid mass region. Thus, to increase the number of detectable peptide ions it was necessary to optimize the MS data resulting in the acquisition of spectra with a high signal to noise ratio in the appropriate mass region. Through these optimizations it was found that a sample matrix consisting of 3 mg/mL CHCA, 8 mM ammonium citrate, 50 % ACN, 0.1 % TFA coupled with an I.D.I. co-crystallization technique resulted in optimal spectra.

A reduction in sample complexity by fractionation increases the probability that all peptides present, regardless of concentration, will be detected due to reduced ion suppression (signal depletion). The peptide landscape of the fractionated samples revealed labeled peptides from 1000 to 2600 (m/z) (Table 3.1) correlating to peptides of

approximately 9-23 aa. The length of the identified peptides is consistent with the size of peptides known to be chaperoned by gp96, which further validates this procedure. It is interesting to note that only one 115-iTRAQ™ labeled peptide, corresponding to a gp96 peptide isolated from the *Homo sapiens* sample, which comprised only 1/10 of the sample, was identified. This may be attributed to the efficiency and effectiveness of the labeling experiment itself or the detection sensitivity of the MS analyzer. As the iTRAQ™ labeling experiment was carried out in tandem with both samples processed at the same time, it is probable that labeling efficiency is not the reason for lack of detection of spiked *Homo sapiens* peptide and we can therefore assume that the detection threshold of the MALDI TOF/TOF analyzer had been reached. Thus a pool of 115-labeled peptides remained present yet undetectable at this concentration in the model sample.

Table 3.1 also highlights an inherent problem with *de novo* sequencing, which impedes comparison of the sequences obtained using various algorithms. Software assisted *de novo* peptide sequencing assigns amino acids to the mass difference between sequential peptide fragments (*y* or *b* ion series) from MS/MS spectrum. The sequence of the peptide is determined by the mass difference between these peaks. Differentiation between amino acids that have identical or nearly identical masses coupled with poor spectra resulting from incomplete fragmentation and/or low signal intensities condemn *de novo* sequencing to an inexact science. Aside from these inherent difficulties, different algorithms have varying amino acid assignment parameters and statistical probability scoring, resulting in sequence discrepancies. For the purpose of the work reported in my thesis, these *de novo* sequences were used to search protein databases for protein identity.

When searching protein databases the user-defined search parameters have a major influence on the successful identification of a fully characterized protein. Both BLAST and Mascot allow the enzyme specificity and number of missed cleavages to be defined in their search criteria yet, because of the nature of the natural peptide sample, these parameters were not relevant. The stringency reduction would tend to increase the number of false positive results. By restricting the database to *Mus musculus* or *Homo sapiens* confidence in the top scoring identities from both algorithms was increased.

A model system was developed to optimize the multi-step procedure leading to the identification of natural peptides chaperoned by gp96 in *T. parva* infected cells. Human (*Homo sapiens* Jurkat) and mouse (*Mus musculus* EL4) cell lines were chosen because human and mouse genome sequences are completed and these sequences are present in non-redundant databases. The gp96 peptides isolated from the mouse cell line were spiked 1:10 with gp96 peptides isolated from the human cell line to model the addition of parasite peptides to the bovine gp96 peptide pool. This model does not address the gp96 expression efficiency of each cell line and only corresponds to the number of cells used in the chaperone isolation process. It is known that both a transformed and a parasite-infected state are considered a stress to T lymphocytes, therefore resulting in an increase in gp96 stress protein expression (Cho et al. 2004; Li et al. 2002). The degree of increase in gp96 expression initiated by either state was not compared due to a limited quantity of the parasite-infected sample. Thus it is reasonable to assume that gp96 isolated from malignant T cell lines may not quantitatively model gp96 isolated from a *T. parva*

infected bovine cell line. However skewed, this model was able to provide proof of concept for the methodology.

Until recently, *T. parva* cell lines have not been allowed into North America. Following substantial safety testing at Plum Island level 4 biosafety laboratory (USA), the level 3 *T. parva* cell lines are currently being held at The Institute for Genomic Research (TIGR) in Rockville MD. Plans are in place to acquire solubilized samples of these cell lines to continue work on this project.

SUMMARY AND CONCLUSIONS

The objective of this study was to develop a procedure to identify potentially antigenic *T. parva* peptides directly from parasite-infected bovine T lymphocytes. Such peptides are potentially immunologically powerful as they become associated with MHC class I molecules forming a complex at the cell surface with the ability to trigger a protective anti-parasitic cell-mediated immune response. Unfortunately, the peptides originating from *T. parva* are diluted in a highly complex mixture of somatic host T lymphocyte peptides, thus sensitive mass spectrometry methods are probably necessary for their identification (Hofmann et al. 2005; Meiring et al. 2006; Torabi-Pour et al. 2003; Zhou et al. 2005). The identification of these peptides is both scientifically and clinically relevant as they will provide insight into a complex century-old relationship between the only eukaryotic parasite known to induce host cell transformation coupled with the potential to establish a strategic approach for a peptide vaccine. This would be based on findings that prove a strong cell-mediated immune response is capable of clearing the bovine host of the intracellular *T. parva* parasites (McKeever et al. 1994; Pearson et al. 1979). Characterization of the MHC-associated *T. parva* peptide antigens is therefore at the crossroads of advanced proteomics and clinically and socioeconomically relevant immunology.

To obtain peptides destined for MHC class I presentation to effector CD 8+ T lymphocytes, my strategy was first to isolate the molecules involved in class I antigen presentation from bovine liver tissue. The MHC class I destined peptides were isolated from soluble ER chaperones rather than the MHC molecule itself as the integrity

compromising isolation methods required to isolate the membrane bound MHC heterodimer would likely result in the loss of the associated antigenic peptides. Conversely, gentle affinity chromatography isolation of the soluble chaperones responsible for shuttling the MHC class I destined peptides within the ER lumen allowed for the retention of their non-covalently associated peptides. Initially, ER specific molecular chaperones were isolated from bovine hepatocytes using traditional biochemical methods. The isolated molecules were used to immunize mice for the generation of monoclonal antibodies (mAbs) specific for molecules involved in the bovine MHC class I antigen-processing pathway.

Although monoclonal antibodies specific to all chaperones of the MHC class I antigen-processing pathway were sought, the most desired target antigen was the soluble ER chaperone gp96. Gp96 does not exclusively function in the assembly of the MHC class I complex; researchers have found that gp96 acts as a potent adjuvant, modulating the CD8⁺ immune response. As a heat shock protein (hsp) within the lumen of the ER, gp96 interacts indiscriminately with the diverse peptide pool destined for association with appropriate MHC class I molecules (Nicchitta et al. 2004). The peptides presented to the immune system on MHC class I molecules must theoretically be biochemically and immunologically similar to the peptides chaperoned by gp96. The elucidation of a mechanism by which gp96 acts as a cell-mediated immune system modulator supports this theory (Srivastava et al. 1994; Udono et al. 1994). Upon necrosis, the typically intracellular chaperone is taken up by antigen presenting cells (APC) through the CD91 receptor. The gp96-chaperoned peptides are released and trafficked through the MHC

class I antigen-processing pathway and displayed as endogenous antigens on the surface of the APC; a phenomenon termed cross presentation. Therefore, these quintessentially intracellular gp96 molecules alert the cell-mediated immune system to pathogen-triggered cell death. Elegantly, the gp96-chaperoned peptides originating from proteins synthesized within the pathogen-harboring cell are presented to the immune system on professional APCs through the process of cross presentation. This allows the antigenic pathogen peptides from the compromised cell to stimulate a protective CD8⁺ immune response. The capacity of gp96 to elicit a CD8⁺ T cell response indicates that this chaperone does in fact bind peptides suitable for assembly in MHC class I molecules. Thus, gp96 was deemed the optimal antigen for monoclonal antibody production as such specific antibodies could be used for immunoaffinity purification of bovine gp96.

Development of monoclonal antibodies against bovine gp96 proved difficult. Multiple fusion techniques were attempted based on literature describing the production of mAbs specific for highly conserved antigens. While mAbs were successfully raised against other members of the soluble ER chaperone assembly, no anti-gp96 mAbs were generated. An anti-gp96 antibody fragment (ScFv) matrix was thus obtained from our collaborator Christian Kleist in Heidelberg and used in the successful optimization of a single step method for the physiological isolation of peptide-associated gp96 chaperones from human, mouse and bovine cell lines. The natural peptides were isolated from the chaperones and derivatized using the primary amine specific iTRAQ™ reagent to allow species-specific comparisons of the infected and non-infected peptide samples by mass spectrometry. A model sample containing mouse gp96 peptides spiked 1:10 with human

gp96 peptides was used to optimize the mass spectrometry analysis and data acquisition for these natural peptides. By increasing the peptide intensity and decreasing the background noise in the relevant mass region, spectra were obtained that gave sequence data and allowed protein identification of several parental mouse proteins. The successful identification of labeled peptides from the model sample encouraged the adaptation of the method to a single sample of *T. parva* infected and uninfected bovine T lymphocyte cell lines. The data obtained revealed few peptides and those present were not iTRAQ™ labeled. It can be surmised that the number of peptides obtained from these samples was not sufficient for detection by the MALDI TOF-TOF. Conceivably, simply increasing the starting cell numbers would allow the identification of *T. parva* peptides from the plethora of bovine peptides chaperoned by bovine gp96 molecules in parasite-infected cells.

FUTURE INVESTIGATION

The remarkable conservation of gp96 throughout evolution coupled with its recently elucidated immune function marks this hsp as a target for pathogen modulation to evade detection by the immune system. Within the recently published *T. parva* genome sequence a parasite gp96 homologue sharing 34% sequence identity to the bovine chaperone was identified (Appendix A). While a housekeeping function provides a reasonable explanation for why gp96 would be encoded by *T. parva*, the chaperone's dual functionality begs the question: is it plausible that the mechanism of immune evasion practiced by *T. parva* parasites is to sequester immunogenic parasitic peptides using the gp96 homologue thereby preventing them from entering the immune response pathway of the infected host animal?

The theory that *Theileria parva* may be using a gp96 homologue to remove immunogenic peptides from the host immune response pathway needs to be entertained. If the host and parasite gp96 both contain the epitope for the anti-gp96 ScFv used in the single step isolation procedure, I will not only be able to identify those peptides interacting with the host immune system but also those peptides specifically sequestered by the parasite. While the pool of retained parasite peptides is of immunological interest they may hinder the identification of *T. parva* peptides presented to the immune system. Regardless of this potential obstacle presented by *T. parva*, the sensitive mass spectrometry based method outlined in the work presented in this thesis may have a great utility in the pursuit

of MHC epitopes useful in vaccination against this diabolical parasite and against many other intracellular pathogens.

APPENDIX ILIST OF ABBREVIATIONS

μ	micro
μL	microlitre
1-D	one dimensional
2-D	two dimensional
1-DGE	1-dimensional gel electrophoresis
2-DGE	2-dimensional gel electrophoresis
A	alanine
aa	amino acids
ACN	acetonitrile
APC	antigen presenting cell
BLAST	basic local alignment search tool
C	cysteine
CD8+	cluster of differentiation
CHCA	alpha-cyano-4-hydroxycinnamic acid
CID	collision-induced dissociation
Con A	concanavalin A
CTL	cytotoxic T lymphocytes
D	aspartate
Da	Dalton
E	glutamate
EDTA	ethylenediaminetetraacetic acid
ELISA	enzyme linked immunosorbant assay
ER	endoplasmic reticulum
F	phenylalanine
g	gravity
G	glycine

H	histidine
HAT	hydroxanthin aminopterin thymidine
HPLC	high performance liquid chromatography
I	isoleucine
iTRAQ™	isobaric tags for relative and absolute quantitation
K	lysine
kDa	kilodalton
L	leucine
m	milli
M	methionine
M	molarity
mg	milligram
mL	millilitre
mAb	monoclonal antibody
MALDI TOF	matrix-assisted laser desorption/ionization time-of-flight
MALDI TOF/TOF	matrix-assisted laser desorption/ionization time-of-flight time-of-flight
MHC	major histocompatibility complex
MS	mass spectrometry
MS/MS	mass spectrometry/mass spectrometry (tandem mass spectrometry)
<i>m/z</i>	mass to charge ratio
N	asparagine
Nd:YAG	neodymium-doped yttrium-aluminum-garnet (laser)
OD	optical density
P	proline
PBS	phosphate buffered saline
PMF	peptide mass fingerprint
PVDF	polyvinylidene difluoride
Q	glutamine
R	arginine
S	serine

SDS	sodium dodecyl sulfate
SDS-PAGE	sodium dodecyl sulfate poly-acrylamine gel electrophoresis
ScFv	single chain fragment variable
T	threonine
TAP	transporter associated with antigen processing
TFA	trifluoroacetic acid
UV	ultraviolet
V	valine
W	tryptophan
Y	tyrosine

APPENDIX II

ALIGNMENT OF ENDOPLASMIC RETICULUM GLYCOPROTEINS
FROM BOVID AND MOUSE

A) CALRETICULIN

B. taurus	MLLPVPLLLGLLGLAAADPTVYFKEQFLDGDGWTERRWIESKHKPDFGKFLVSSGKIFYGDQ	60
M. musculus	MLLSVPLLLGLLGLAAADPAIYFKEQFLDGDGAWTNRWVESKHKSDFGKFLVSSGKIFYGDL	60
	.**:*****.**:**:*:**.*****.*****	
B. taurus	EKDKGLQTSQDARFYALSARFEPFSNKGQTLVVQFTVKHEQNIDCGGGYVKLFPAGLDQT	120
M. musculus	EKDKGLQTSQDARFYALSARFEPFSNKGQTLVVQFTVKHEQNIDCGGGYVKLFPAGLDQK	120
	*****:*****:*****.*****.*****	
B. taurus	DMHGDSEYNIMFGPDICGPGTKKVHVIFNYKGKNVLINKDIRCKDDEFTHLYTLIVRPNN	180
M. musculus	DMHGDSEYNIMFGPDICGPGTKKVHVIFNYKGKNVLINKDIRCKDDEFTHLYTLIVRPDN	180
	*****:*****:*****.*****.*****	
B. taurus	TYEVKIDNSQVESGSLEDDWDFLPPKKIKDPDAAKPEDWDDRAKIDDPDTSKPEDWDKPE	240
M. musculus	TYEVKIDNSQVESGSLEDDWDFLPPKKIKDPDAAKPEDWDERAKIDDPDTSKPEDWDKPE	240
	*****:*****:*****.*****.*****	
B. taurus	HIPDPDAKKPEDWDEEMDGEWEPPIQNPEYKGEWKPRQIDNPEYKGIWIHPEIDNPEYS	300
M. musculus	HIPDPDAKKPEDWDEEMDGEWEPPIQNPEYKGEWKPRQIDNPDYKGTWIHPEIDNPEYS	300
	*****:*** *****	
B. taurus	PDSNIYAYENFAVLGLDLWQVKSGETIFDNFLITNDEAYAEFFGNETWGVTKAAEKQMKDK	360
M. musculus	PDANIYAYDSFAVLGLDLWQVKSGETIFDNFLITNDEAYAEFFGNETWGVTKAAEKQMKDK	360
	:*::*****:*****.*****.*****	
B. taurus	QDEEQRLHEEEEEKKGKEEEEAD-KDDDEDKDEDEDEDEKEEEEEEDAAAGQAKDEL	417
M. musculus	QDEEQRLKEEEEDKKRKEEEEAEKEDDDDRDEDEDEDEKEEEDDEE--SPGQAKDEL	416
	*****:***:* *****: **:*:**:*****:*****:*** :.*****	

B) GP96

B. taurus	MRALWVLGLCCVLLTFGFSVRADDEVDVDGTVEEDLGKSREGSRTDDEVVQREEEAIQLDG	60
M. musculus	MRVLWVLGLCCVLLTFGFVRADEVDVDGTVEEDLGKSREGSRTDDEVVQREEEAIQLDG	60
	** .*****	
B. taurus	LNASQIRELREKSEKFAFQAEVNRMMKLIINSLYKNKEIFLRELISNASDALDKIRLISL	120
M. musculus	LNASQIRELREKSEKFAFQAEVNRMMKLIINSLYKNKEIFLRELISNASDALDKIRLISL	120

B. taurus	TDENALAGNEELTVKIKCDKEKNLLHVTDTGVMGTREELVKNLGTIAKSGTSEFLNKMTE	180
M. musculus	TDENALAGNEELTVKIKCDKEKNLLHVTDTGVMGTREELVKNLGTIAKSGTSEFLNKMTE	180

B. taurus	AQEDGQSTSELIGQFGVGFYSAFLVADKVIIVTSKHNNDTQHIWESDSNEFSVIADPRGNT	240
M. musculus	AQEDGQSTSELIGQFGVGFYSAFLVADKVIIVTSKHNNDTQHIWESDSNEFSVIADPRGNT	240

B. taurus	LGRGTTITLVLKEEASDYLELDTIKNLVKKYSQFINFPIYVWSSKTEVVEEPAEEEEAAK	300
M. musculus	LGRGTTITLVLKEEASDYLELDTIKNLVKKYSQFINFPIYVWSSKTEVVEEPLLEDEAAK	300
	*****:***** **:	
B. taurus	EDKEESDDEAAVEEEEEDEKPKTKKVEKTVWDWELMNDIKPIWQRPSKEVEEYKAFYK	360
M. musculus	EEKEESDDEAAVEEEEEDEKPKTKKVEKTVWDWELMNDIKPIWQRPSKEVEEYKAFYK	360
	*:*****:*****	
B. taurus	SFSKESDDPMAYIHFTAEGEVTFKSILFVPTSAPRGLFDEYGSKKSDYIKLYVRRVFTD	420
M. musculus	SFSKESDDPMAYIHFTAEGEVTFKSILFVPTSAPRGLFDEYGSKKSDYIKLYVRRVFTD	420

B. taurus	DFHDMMPKYLNFVKGVDSDDLPLNVSRETQQHKLKLVIRKLVKRLDLMIKKIADKDY	480
M. musculus	DFHDMMPKYLNFVKGVDSDDLPLNVSRETQQHKLKLVIRKLVKRLDLMIKKIADKDY	480

B. taurus	NDTFWKEFGTNIKLGVIEDHSNRTRLAKLLRFQSSHHPSDMTSLDQYVERMKEKQDKIYF	540
M. musculus	NDTFWKEFGTNIKLGVIEDHSNRTRLAKLLRFQSSHHSTDIITSLDQYVERMKEKQDKIYF	540
	*****.:*****	
B. taurus	MAGASRKEAESSPFVERLLKKGYEVIYLTPEVDEYCIQALPEFDGKRFQNVAKGKVFDE	600
M. musculus	MAGSSRKEAESSPFVERLLKKGYEVIYLTPEVDEYCIQALPEFDGKRFQNVAKGKVFDE	600
	:**	
B. taurus	SEKSKESREAVEKEFEPLLNWMKDKALKDKIEKAVVSQRLTESPCALVASQYGSNGMER	660
M. musculus	SEKTKESREATEKEFEPLLNWMKDKALKDKIEKAVVSQRLTESPCALVASQYGSNGMER	660
	:**	
B. taurus	IMKAQAYQTGKDI STNYASQKKTFEINPRHPLIRDMLRRVKEDEDDKTVSDLAVVLFET	720
M. musculus	IMKAQAYQTGKDI STNYASQKKTFEINPRHPLIRDMLRRIKEDDDKTVMDLAVVLFET	720
	*****:*****	
B. taurus	ATLRSGYLLPDTKAYGDRIERMLRSLNIDPDAKVEEPEEPEETTEDTAEDTEQDEEE	780
M. musculus	ATLRSGYLLPDTKAYGDRIERMLRSLNIDPEAQVEEPEEPEEDTSED-AEDSEQDEGE	779
	*****:*****:*** **:	
B. taurus	EMDAGTDEEEQETAEKSTA EKDEL	804
M. musculus	EMDAGTEEEET-EKESTEKDEL	802
	*****:***:*** **.:*****	

APPENDIX III

ALIGNMENT OF BOVID AND *T. parva* GP96

<i>B. taurus</i>	-MRALWVLGLCCVLLTFG--SVRADDEVVDVGTVEEDLGKSREGSRTDDEVVQREEEAIQ	57
<i>T. parva</i>	MNISLFLRLRILFILYLSRGDNFAFCDESDDLVVEDPVSFDEIKVEDEAPAALSEEELLD	60
	:*:* * * :* .. ** * .** :. . . : .. *** :	
<i>B. taurus</i>	LDG---LNASQIRELREKSEKFAFQAEVNRMMKLIINSLYKNKEIFLRELI SNASDALD	113
<i>T. parva</i>	MSEDSSVLTSEKLFKDSAKSEKYEYQAEVTRLDIIVNSLYSSKDIPLRELVNSADALE	120
	:. * :. :. : * * * : * * * : * * * : * * * : * * * : * * * : * * * :	
<i>B. taurus</i>	KIRLISLTDENALAGNEELTVKIKCDKEKNLLHVTDTGVGMTREELVKNLGTIAKSGTSE	173
<i>T. parva</i>	KYKITALQKN-YKDKDVELFVRIRSYPKRLLTIWDNGVGMTKSELMNLTIAKSGTAN	179
	* :. : * . : : * * * : * * * : * * * : * * * : * * * : * * * : * * * :	
<i>B. taurus</i>	FLNKMTEAQEDGQSTSELIGQFVGFYSAFLVADKVIIVTSKHNNDTQHIWESDSNEFSVI	233
<i>T. parva</i>	FLDLSKVGND---PNLIGQFVGFYSAFLVADTVLVQSKNYEDKQYVWRSSAANSYEL	235
	** :. :. :. : * . : * :	
<i>B. taurus</i>	ADPRGNTLG-RGTTITLVLKEEASDYLELDTIKNLVKKYSQFINFPIYVWSSKTETVEEP	292
<i>T. parva</i>	YEDTDNSLGDHGTITLLELREDATDYLKTDLVLENLVKKYSQFVKYPIQLYK-----	286
	: . * : * :	
<i>B. taurus</i>	AEEEEAAKEDKEESDDEAAVEEEDEKPKTKKVEKTVDWELMNDIKPIWQPSKEVEE	352
<i>T. parva</i>	-----KLKDKQELGWVKNETQQIWTNRKNTITE	315
	* : * :	
<i>B. taurus</i>	DEYKAFYKFSKESDDPMAYIHFTAEGEVTFKSI LFPVTSAPRGLFDEYGSKKS DYIKLY	412
<i>T. parva</i>	QEYNEFYKTI SGTDEPLAHVHFTAEGVDVFKALLYIPSSPPAMYFSSSVGHN--VKLY	373
	: * * : * * * : * : * :	
<i>B. taurus</i>	VRRVFITDDFDMMPKYLNLFVKGVDSDDLPLNVSRETLQQHKLLKVKIRKLVKRTLDMI	472
<i>T. parva</i>	SRRVLVSQEMRDFIPRYLFSVGVVSDSFPLNVSREYLQQSKLVKLI GKKVVRTVLDL	433
	* * * :. :. :. : * : * :	
<i>B. taurus</i>	KKIADKEYNDT-----	483
<i>T. parva</i>	YDVMKKSIEDVKEVEDELEKVKSVKEKEWNTYKDKWKKRNDKEFKEFELSSKNQRDKEE	493
	. : . : * * * :	
<i>B. taurus</i>	-----FWKEFGTNIKLVIEDHSNR	503
<i>T. parva</i>	NMEDNEKNKKGKSLWSADVELRRKLEKRLKEVDRYSKFYNGFKGSLKVCYDDDDQNR	553
	* : * * . : * :	
<i>B. taurus</i>	TRLAKLLRFQSSHHPDMSLDQYVERMKEKQDKIYFMAGASRKEAESSPFVERLLKKG	563
<i>T. parva</i>	KKIARLLRYKTLFSEKELT-FDEYVDKMPPEQTEIYVVTSESYEDLKQMPHLQGLKRRKF	612
	. : * * * * * : . : * * : * :	
<i>B. taurus</i>	EVIYLTPEVDEYCIQALPEFDGKRFQVAKGKVFDESEKSKESREAVEKEFEPELLNWMK	623
<i>T. parva</i>	DVLYLHDTMDEGLTKLEEHGRKFKVQKADLNLKLTDEEQKEERKETKYKPLILYLK	672
	: * * * :. : * :	
<i>B. taurus</i>	DKALKDKIEKAVVSQRLETSPCALVASQYGSNGMERIMKAQAYQTGKDI STNYYASQKK	683
<i>T. parva</i>	D--LLPETSGVLSRRLVEDPCTVVASEWSMSSHMEKLMKSYAVHR--DSDPDMFNKLNK	729
	* * : . . : * :	
<i>B. taurus</i>	TFEINPRHPLIRDMLRRVKE-----	703
<i>T. parva</i>	VLELNPDPHPI MVKLLYLTQTQKLDQRNDTERVEKERQKQDTEGEKDTGEKDTGEKDS	789
	. : * * * * * : . : * * . : :	
<i>B. taurus</i>	--DEDDKTVSD-----LAVVLFETATLRSGYLLPDT-----	732
<i>T. parva</i>	EREEDKKTDDQSTDVERRELLERKSRYMRRDLRFLKLLYNAAKLKS GFVLEEPQLVVNY	849
	: * * * . : * :	
<i>B. taurus</i>	-----KAYGDRIERMLRSLNIDPDAKVEEPEEPEP-----EET	766
<i>T. parva</i>	LYEKLNRSLGDFVERDFEF SKNLTLDDEVDKVVETPVPEHLKMQLEMESQTQGTQS	909
	: : * * * * * : . : * * * * * : : * * * * * : :	
<i>B. taurus</i>	TEDTAEDTEQDEEEEMDAGTDEEEQETAEKSTA EKDEL-----	804
<i>T. parva</i>	TEGSTGTEGSTGTDTKSTQSTETESPEPKSPEEKGMDDGLELEEIFAGKDPGFEVTR	969
	* * :. : * * . . . * :. : * * * * * :. : * * * * * :	
<i>B. taurus</i>	-----	
<i>T. parva</i>	GSVDDAEEGEQAMFDHLKSRGLDVEKLRSKQEDYDWSNDEL	1009

BIBLIOGRAPHY

- Arnold, D., Faath, S., Rammensee, H. and Schild, H., Cross-priming of minor histocompatibility antigen-specific cytotoxic T cells upon immunization with the heat shock protein gp96, *Journal of Experimental Medicine*, 182 (1995) 885-9.
- Association, C.o.F.A.D.o.t.U.S.A.H., Foreign Animal Diseases "The Grey Book", Pat Campbell & Associates and Carter Printing Company, 1998a.
- Association, U.S.A.H., Foreign Animal Diseases, Pat Campbell & Associates, 1998b, 432 pp.
- Baldwin, C.L., Malu, M.N. and Grootenhuis, J.G., Evaluation of cytotoxic lymphocytes and their parasite strain specificity from African buffalo infected with *Theileria parva*, *Parasite Immunology*, 10 (1988) 393-403.
- Beecroft, R.P., Roditi, I. and Pearson, T.W., Identification and characterization of an acidic major surface glycoprotein from procyclic stage *Trypanosoma congolense*, *Molecular and Biochemical Parasitology*, 61 (1993) 285-94.
- Bishop, R., Lambson, B., Wells, C., Pandit, P., Osaso, J., Nkonge, C., Morzaria, S., Musoke, A. and Nene, V., A cement protein of the tick *Rhipicephalus appendiculatus*, located in the secretory cell granules of the type III salivary gland acini, induces strong antibody responses in cattle, *International Journal for Parasitology*, 32 (2002) 833-42.
- Blachere, N.E., Li, Z., Chandawarkar, R.Y., Suto, R., Jaikaria, N.S., Basu, S., Udono, H. and Srivastava, P.K., Heat shock protein-peptide complexes, reconstituted in vitro, elicit peptide-specific cytotoxic T lymphocyte response and tumor immunity, *Journal of Experimental Medicine*, 186 (1997) 1315-22.
- Blachere, N.E., Udono, H., Janetzki, S., Li, Z., Heike, M. and Srivastava, P.K., Heat shock protein vaccines against cancer, *Journal of Immunotherapy*, 14 (1993) 352-6.
- Boes, M., Prodeus, A.P., Schmidt, T., Carroll, M.C. and Chen, J., A critical role of natural immunoglobulin M in immediate defense against systemic bacterial infection, *Journal of Experimental Medicine*, 188 (1998) 2381-6.

- Brams, P., Pettijohn, D.E., Brown, M. and Olsson, L., In vitro B-lymphocyte antigen priming against both non-immunogenic and immunogenic molecules requiring low amounts of antigen and applicable in hybridoma technology, *Journal of Immunological Methods*, 98 (1987) 11-22.
- Chirmule, N., Current advances in molecular immunology: reference guide for reviews on molecular vaccines, *Frontiers in Bioscience*, 9 (2004) 2373-87.
- Cho, N.H., Choi, C.Y. and Seong, S.Y., Down-regulation of gp96 by *Orientia tsutsugamushi*, *Microbiology and Immunology*, 48 (2004) 297-305.
- Cranefield, P., *Science and Empire: East Coast fever in Rhodesia and the Transvaal.*, Cambridge University Press, 1991, 385 pp.
- Dobbelaere, D.A., Fernandez, P.C. and Heussler, V.T., *Theileria parva*: taking control of host cell proliferation and survival mechanisms, *Cellular Microbiology*, 2 (2000) 91-9.
- Dolan, T.T., Dogmas and misunderstandings in East Coast fever, *Tropical Medicine & International Health*, 4 (1999) A3-11.
- Goding, J.W., *Monoclonal Antibodies: Principle and Practice.*, Academic Press, London, 1983.
- Gromme, M. and Neefjes, J., Antigen degradation or presentation by MHC class I molecules via classical and non-classical pathways, *Molecular Immunology*, 39 (2002) 181-202.
- Haddow, J.D., Poulis, B., Haines, L.R., Gooding, R.H., Aksoy, S. and Pearson, T.W., Identification of major soluble salivary gland proteins in teneral *Glossina morsitans morsitans*, *Insect Biochemistry and Molecular Biology*, 32 (2002) 1045-53.
- Heike, M., Blachere, N.E. and Srivastava, P.K., Protective cellular immunity against a spontaneous mammary carcinoma from ras transgenic mice, *Immunobiology*, 190 (1994) 411-23.

- Heussler, V.T., Rottenberg, S., Schwab, R., Kuenzi, P., Fernandez, P.C., McKellar, S., Shiels, B., Chen, Z.J., Orth, K., Wallach, D. and Dobbelaere, D.A., Hijacking of host cell IKK signalosomes by the transforming parasite *Theileria*, *Science*, 298 (2002) 1033-6.
- Hofmann, S., Gluckmann, M., Kausche, S., Schmidt, A., Corvey, C., Lichtenfels, R., Huber, C., Albrecht, C., Karas, M. and Herr, W., Rapid and sensitive identification of major histocompatibility complex class I-associated tumor peptides by Nano-LC MALDI MS/MS, *Molecular and Cellular Proteomics*, 4 (2005) 1888-97.
- Honda, Y., Matsubara, Y., Morzaria, S. and McKeever, D., Immunohistochemical detection of parasite antigens in *Theileria parva*-infected bovine lymphocytes, *Veterinary Parasitology*, 80 (1998) 137-47.
- Johnson, R.S., Davis, M.T., Taylor, J.A. and Patterson, S.D., Informatics for protein identification by mass spectrometry, *Methods*, 35 (2005) 223-36.
- Kaufmann, J., *Parasitic Infections of Domestic Animals: a diagnostic manual.*, Birkhauser Verlag, 1996.
- Kuby, J., *Immunology Third Edition*, W. H. Freeman and Company, 1997.
- Li, Z., Dai, J., Zheng, H., Liu, B. and Caudill, M., An integrated view of the roles and mechanisms of heat shock protein gp96-peptide complex in eliciting immune response, *Frontiers in Bioscience*, 7 (2002) d731-51.
- Linderoth, N.A., Simon, M.N., Rodionova, N.A., Cadene, M., Laws, W.R., Chait, B.T. and Sastry, S., Biophysical analysis of the endoplasmic reticulum-resident chaperone/heat shock protein gp96/GRP94 and its complex with peptide antigen, *Biochemistry*, 40 (2001) 1483-95.
- Liu, C., Ewing, N. and DeFilippo, M., Analytical challenges and strategies for the characterization of gp96-associated peptides, *Methods*, 32 (2004) 32-7.
- Ma, M., Wu, S., Howard, M., and Borkovec, A., Enhanced production of mouse hybridomas to picomoles of antigen using EL-4 conditioned media with an in vitro immunization protocol., *In vitro*, 20 (1984) 739.

- Macdonald-Levy, M., MacMillan, S., International Livestock Research Institute., Vol. 2006, 2005.
- Marcotty, T., Brandt, J., Billiouw, M., Chaka, G., Losson, B. and Berkvens, D., Immunisation against *Theileria parva* in eastern Zambia: influence of maternal antibodies and demonstration of the carrier status, *Veterinary Parasitology*, 110 (2002) 45-56.
- Matsuoka, K., Seta, K., Yamakawa, Y., Okuyama, T., Shinoda, T. and Isobe, T., Covalent structure of bovine brain calreticulin, *Biochemical Journal*, 298 (Pt 2) (1994) 435-42.
- McKeever, D.J., Cellular immunity against *Theileria parva* and its influence on parasite diversity, *Research in Veterinary Science*, 70 (2001) 77-81.
- McKeever, D.J. and Morrison, W.I., Novel vaccines against *Theileria parva*: prospects for sustainability, *International Journal for Parasitology*, 28 (1998) 693-706.
- McKeever, D.J., Taracha, E.L., Innes, E.L., MacHugh, N.D., Awino, E., Goddeeris, B.M. and Morrison, W.I., Adoptive transfer of immunity to *Theileria parva* in the CD8+ fraction of responding efferent lymph, *Proceedings of the National Academy of Sciences of the United States of America*, 91 (1994) 1959-63.
- Meiring, H.D., Soethout, E.C., Poelen, M.C., Mooibroek, D., Hoogerbrugge, R., Timmermans, H., Boog, C.J., Heck, A.J., de Jong, A.P. and van Els, C.A., Stable isotope tagging of epitopes-a highly selective strategy for the identification of MHC class I-associated peptides induced upon viral infection, *Molecular and Cellular Proteomics* (2006).
- Meng, S.D., Song, J., Rao, Z., Tien, P. and Gao, G.F., Three-step purification of gp96 from human liver tumor tissues suitable for isolation of gp96-bound peptides, *Journal of Immunological Methods*, 264 (2002) 29-35.
- Morzaria, S., Nene, V., Bishop, R. and Musoke, A., Vaccines against *Theileria parva*, *Annals of the New York Academy of Sciences*, 916 (2000) 464-73.
- Neuhoff, V., Arold, N., Taube, D. and Ehrhardt, W., Improved staining of proteins in polyacrylamide gels including isoelectric focusing gels with clear background at nanogram sensitivity using Coomassie Brilliant Blue G-250 and R-250, *Electrophoresis*, 9 (1988) 255-62.

- Nicchitta, C.V., Carrick, D.M. and Baker-Lepain, J.C., The messenger and the message: gp96 (GRP94)-peptide interactions in cellular immunity, *Cell Stress & Chaperones*, 9 (2004) 325-31.
- Norval, R.A.I., Perry, B.D. and Young, A.S., *The epidemiology of Theileriosis in Africa*, Academic Press Limited, 1992.
- Pamer, E. and Cresswell, P., Mechanisms of MHC class I--restricted antigen processing, *Annual Review of Immunology*, 16 (1998) 323-58.
- Paquet, M.E. and Williams, D.B., Mutant MHC class I molecules define interactions between components of the peptide-loading complex, *International Immunology*, 14 (2002) 347-58.
- Paulsson, K. and Wang, P., Chaperones and folding of MHC class I molecules in the endoplasmic reticulum, *Biochimica et Biophysica Acta*, 1641 (2003) 1-12.
- Pearson, E.b.T.W., *Parasite Antigens. Toward new strategies for vaccines.*, Vol. 7, Marcel Dekker, Inc., 1986, 413 pp.
- Pearson, T.W., Lundin, L.B., Dolan, T.T. and Stagg, D.A., Cell-mediated immunity to Theileria-transformed cell lines, *Nature*, 281 (1979) 678-80.
- Pinstrup-Anderson, P., Pandya-Lorch, R., et al, *World Food Prospects: Critical Issues for the Early Twenty-first Century.*, Washington, DC, 1999.
- Purcell, A.W. and Gorman, J.J., Immunoproteomics: Mass spectrometry-based methods to study the targets of the immune response, *Molecular and Cellular Proteomics*, 3 (2004) 193-208.
- Rosegrant, M.W. and Cline, S.A., Global food security: challenges and policies, *Science*, 302 (2003) 1917-9.
- Sastry, S. and Linderoth, N., Molecular mechanisms of peptide loading by the tumor rejection antigen/heat shock chaperone gp96 (GRP94), *Journal of Biological Chemistry*, 274 (1999) 12023-35.

- Shaw, M.K., Cell invasion by *Theileria* sporozoites, *Trends in Parasitology*, 19 (2003) 2-6.
- Spee, P. and Neefjes, J., TAP-translocated peptides specifically bind proteins in the endoplasmic reticulum, including gp96, protein disulfide isomerase and calreticulin, *European Journal of Immunology*, 27 (1997) 2441-9.
- Srivastava, P.K., Purification of heat shock protein-peptide complexes for use in vaccination against cancers and intracellular pathogens, *Methods*, 12 (1997) 165-71.
- Srivastava, P.K., Udono, H., Blachere, N.E. and Li, Z., Heat shock proteins transfer peptides during antigen processing and CTL priming, *Immunogenetics*, 39 (1994) 93-8.
- Tolson, D.L., Turco, S.J., Beecroft, R.P. and Pearson, T.W., The immunochemical structure and surface arrangement of *Leishmania donovani* lipophosphoglycan determined using monoclonal antibodies, *Molecular and Biochemical Parasitology*, 35 (1989) 109-18.
- Torabi-Pour, N., Morrow, W.J., Saffie, R., Gowda, P.G., Perrett, D. and Oliver, T.R., Identification and quantification of antigens associated with HLA class I molecules on a bladder tumour cell line. Implications for vaccine design, *Urologia Internationalis*, 70 (2003) 154-60.
- Udono, H., Levey, D.L. and Srivastava, P.K., Cellular requirements for tumor-specific immunity elicited by heat shock proteins: tumor rejection antigen gp96 primes CD8⁺ T cells in vivo, *Proceedings of the National Academy of Sciences of the United States of America*, 91 (1994) 3077-81.
- Uilenberg, G., Immunization against diseases caused by *Theileria parva*: a review, *Tropical Medicine & International Health*, 4 (1999) A12-20.
- Uilenberg, G., Dobbelaere, D.A., de Gee, A.L. and Koch, H.T., Progress in research on tick-borne diseases: theileriosis and heartwater, *Veterinary Quarterly*, 15 (1993) 48-54.
- von Bonin, A., More, S.H. and Breloer, M., Purification of the eucaryotic heat-shock proteins Hsp70 and gp96, *Methods in Molecular Biology*, 215 (2003) 193-200.

- Watt, D.M. and Walker, A.R., Pathological effects and reduced survival in *Rhipicephalus appendiculatus* ticks infected with *Theileria parva* protozoa, *Parasitology Research*, 86 (2000) 207-14.
- Yewdell, J.W., Reits, E. and Neefjes, J., Making sense of mass destruction: quantitating MHC class I antigen presentation, *Nature Reviews Immunology*, 3 (2003) 952-61.
- Zhou, M., Peng, J.R., Zhang, H.G., Wang, H.X., Zhong, Z.H., Pan, X.Y., Chen, W.F. and Leng, X.S., Identification of two naturally presented MAGE antigenic peptides from a patient with hepatocellular carcinoma by mass spectrometry, *Immunology Letters*, 99 (2005) 113-21.
- Zhu, X. and Papayannopoulos, I.A., Improvement in the detection of low concentration protein digests on a MALDI TOF/TOF workstation by reducing alpha-cyano-4-hydroxycinnamic acid adduct ions, *Journal of Biomolecular Techniques*, 14 (2003) 298-307.